Published in final edited form as:
Dent Mater. 2014 January ; 30(1): . doi:10.1016/j.dental.2013.07.013.

Biomimetic remineralization of dentin

Li-na Niu[1,*], **Wei Zhang**[2,*], **David H. Pashley**[3], **Lorenzo Breschi**[4], **Jing Mao**[2], **Ji-hua Chen**[1,¶], and **Franklin R. Tay**[3,5,¶]

[1]Department of Prosthodontics, School of Stomatology, Fourth Military Medical University, Xi'an, China

[2]Department of Stomatology, Tongji Hospital, Huazhong University of Science and Technology, Wuhan, China

[3]Department of Oral Biology, Georgia Regents University, Augusta, Georgia, USA

[4]Department of Medical Sciences, University of Trieste, Trieste and IGM-CNR, Bologna, Italy

[5]Department of Endodontics, Georgia Regents University, Augusta, Georgia, USA

Abstract

Objectives—Remineralization of demineralized dentin is important for improving dentin bonding stability and controlling primary and secondary caries. Nevertheless, conventional dentin remineralization strategy is not suitable for remineralizing completely-demineralized dentin within hybrid layers created by etch-and-rinse and moderately aggressive self-etch adhesive systems, or the superficial part of a caries-affected dentin lesion left behind after minimally invasive caries removal. Biomimetic remineralization represents a different approach to this problem by attempting to backfill the demineralized dentin collagen with liquid-like amorphous calcium phosphate nanoprecursor particles that are stabilized by biomimetic analogs of noncollagenous proteins.

Methods—This paper reviewed the changing concepts in calcium phosphate mineralization of fibrillar collagen, including the recently discovered, non-classical particle-based crystallization concept, formation of polymer-induced liquid- precursors (PILP), experimental collagen models for mineralization, and the need for using phosphate-containing biomimetic analogs for biomimetic mineralization of collagen. Published work on the remineralization of resin-dentin bonds and artificial caries-like lesions by various research groups was then reviewed. Finally, the problems and progress associated with the translation of a scientifically-sound concept into a clinically-applicable approach are discussed.

Results and Significance—The particle-based biomimetic remineralization strategy based on the PILP process demonstrates great potential in remineralizing faulty hybrid layers or caries-like dentin. Based on this concept, research in the development of more clinically feasible dentin remineralization strategy, such as incorporating poly(anionic) acid-stabilized amorphous calcium phosphate nanoprecursor-containing mesoporous silica nanofillers in dentin adhesives, may

Corresponding authors: Franklin R. Tay, Georgia Regents University, Augusta, Georgia, 30912-1129, USA. TEL: (706) 7212031; ftay@gru.edu; Jihua Chen, School of Stomatology, Fourth Military Medical University, Xi'an, China; jhchen@fmmu.edu.cn.
*Equal contributors
¶Co-corresponding authors

provide a promising strategy for increasing of the durability of resin-dentin bonding and remineralizing caries-affected dentin.

Keywords

Biomimetic; Mineralization; Dentin

1 Introduction

Teeth are the most heavily mineralized tissues in the human body. Demineralization and remineralization processes coexist in teeth during the entire life of an individual. In pathological conditions, demineralization outweighs remineralization [1]. Fermentation of dietary carbohydrates by acidogenic bacteria results in the production of acids such as lactic acid, acetatic acid and propionic acid that demineralize enamel and dentin. As the carious lesion progresses into dentin, activation of endogenous, bound matrix metalloproteinases and cysteine cathepsins will lead to the degradation of collagen fibrils and decrease in the mechanical properties of dentin [2,3]. Prevention and treatment of dental caries is a major challenge because as many as nine out of ten adults in Western countries suffer from dental caries [4]. In the United States alone, more than 100 million dollars is spent annually on dental service. Despite significant advances in preventive and restorative dentistry, replacement of tooth fillings constitutes a substantial share of this annual dental expenditure, due to limited durability of contemporary resin-based restorative materials, particularly when these materials are applied to damaged dentin in the absence of a superficial enamel layer [5–7].

Apart from caries, resin-dentin bonding is another major reason for dentin demineralization [8]. The formation of resin-dentin bonds is accomplished predominantly by micromechanical retention via resin penetration and entanglement of exposed collagen fibrils in the partially or completely demineralized dentin. This is achieved by etching dentin with acids or acidic resin monomers derived from self-etching primers/adhesives to expose the collagen fibrils [7]. To date, it is impossible for resin monomers to completely displace water within the extrafibrillar and particularly the intrafibrillar compartments of a demineralized collagen matrix, and infiltrate the collagen network completely [8–10]. Even if this may be achieved, the limited intermolecular space (1.26–1.33 nm) between collagen molecules renders it challenging to accommodate even small, extended resin monomer molecules such as triethyleneglycol dimethacrylate (≈ 2 nm long) [11]. This invariably results in the presence of mineral-depleted, resin-sparse, water-rich collagen fibrils along the bonded interface [7,9]. Under the combined challenges of enzymes, temperature and functional stresses, regions of incomplete resin infiltration within the dentin hybrid layer is susceptible to degradation, resulting in damage of interfacial integrity, reduction in bond strength and ultimately, the failure of resin-dentin bonds. Thus, remineralization of demineralized dentin has important consequences for control of dentinal caries as well as improvement of dentin bonding stability [8,10].

Different strategies have been employed for remineralizing demineralized dentin. For instance, fluoride, amorphous calcium phosphate (ACP)-releasing resins or resin-based adhesives containing bioactive glass have been used to improve the resistance of bonded restorations to secondary caries [12–15] However, most of these studies focused on remineralizing partially-demineralized carious dentin, which was based on the epitaxial deposition of calcium and phosphate ions over existing apatite seed crystallites [16]. With these traditional ion-based strategies, remineralization does not occur in locations where seed crystallites are absent [17]. Thus, the classical ion-based crystallization concept may not be applicable for remineralizing completely-demineralized dentin within hybrid layers

created by etch-and-rinse adhesive systems or the superficial part of a caries-affected dentin lesion left behind after minimally invasive caries removal, due to the unavailability of seed crystallites in those regions for accomplishing homogeneous nucleation of apatite crystallites [18,19].

Biomimetic remineralization represents a different approach to this problem by attempting to backfill the demineralized dentin collagen with liquid-like ACP nanoprecursor particles that are stabilized by biomimetic analogs of noncollagenous proteins [20–22]. This is achieved by adopting the recently discovered, non-classical particle-based crystallization concept utilized by Nature in various biomineralization schemes, ranging from the mineralization of sea-shells (calcium carbonate), siliceous shells of diatoms and sponges (amorphous silica) to the deposition of calcium phosphate salts in fish scales and bone [23,24]. Intrafibrillar mineralization of fibrillar collagen not only significantly increases its mechanical properties [25–28], but also protects the collagen molecules from external challenges, such as temperature, endogenous enzymes, bacterial acids and other chemical factors. Using this biomimetic remineralization strategy, both hybrid layers created by etch-and-rinse adhesives [21,29,30] and moderately aggressive self-etch adhesives [18,31,32], as well as 250–300 μm thick completely demineralized dentin lesions can be remineralized [33,34]. This bottom-up remineralization strategy does not rely on seed crystallites, and may be considered as a potentially useful mechanism in extending the longevity of resin-dentin bonds [35] via restoring the dynamic mechanical properties of the denuded collagen within the hybrid layer to approximate those of mineralized dentin [36]. This paper reviews the changing concepts in calcium phosphate remineralization and the progress in clinical translation of the biomimetic dentin remineralization strategy.

2 Changing Concepts of Calcium Phosphate Biomineralization

Biomineralization is the process by which living organisms secrete inorganic minerals in the form of biominerals (e.g. magnetite, silica, oxalates, various crystalline forms of calcium carbonate and carbonated apatite) within cell cytoplasm, shells, teeth and bony skeletons [37,38]. This process exhibits a high level of spatial and hierarchical control as mineralization usually takes place in a confined reaction environment under ambient temperature and pressure conditions. Calcified human tissues consist of the collagen matrix and the hierarchically-arranged carbonated apatite inorganic phase; deposition of the latter is regulated by noncollagenous proteins [39,40]. It is generally believed that non-collagenous proteins, along with specific MMPs and other important enzymes secreted by odontoblasts, play critical roles to orchestrate dentin mineralization. They possess carboxylic acid and phosphate functional groups that act as preferential sites for Ca/P nucleation and subsequent apatite crystallization [41–43]. As the therapeutic use of native or recombinant non-collagenous proteins for in situ biomineralization is not yet economically viable, research scientists have resorted to the use of polyelectrolyte and poly(acid) macromolecules to mimic the functional domains of these naturally-occurring proteins, in biomimetic mineralization [44–47]. In the past few years, this field of research has attracted a lot of attention, resulting in changing concepts of calcium phosphate biomineralization.

2.1 Particle-based vs ion-based crystallization

Traditional collagen mineralization studies were based on the classical pathway of ionmediated crystallization, or classical nucleation theory [37,48]. The classical model of crystal formation begins with crystal nucleation, followed by crystal growth. This process starts from primary building blocks like atoms, ions or molecules, forming clusters, which may grow or disintegrate again, depending on the counter-play of surface and crystal lattice energies. Eventually, some clusters reach the size of a so-called critical crystal nucleus. These primary nuclei grow further via ion-by-ion attachment and unit cell replication. While

the classical crystallization model was relatively successful in controlling the dimensions of calcium carbonate or calcium phosphate, they achieved limited success in reproducing the structural hierarchy of intrafibrillar apatite deposition [49] within the collagen matrix.

In contrast to the ion-mediated classical crystallization pathway, the non-classical crystallization pathway is particle-mediated and involves a mesoscopic transformation process [22,50]. The term mesoscopic refers to materials of an intermediate length scale, the lower limit may be the size of individual atoms. Whereas macroscopic objects usually obey the laws of classical mechanics, a large number of particles can interact in a quantum-mechanically correlated fashion for mesoscopic objects. Evidence for these pathways is rapidly increasing in the literature. To date, mesocrystals of a wide range of materials including $CaCO_3$, $BaSO_4$, metal oxides, metal tungstates and chromates, NH_4TiOF_3, $(NH_4)_3PW_{12}O_{40}$, $LiFePO_4$, metal chalcogenides (e.g. semiconductor cadmium sulphide), noble metals, and organic materials have been successfully synthesized, as described in several excellent reviews [23,51]. The contemporary concept of calcium phosphate biomineralization has been advanced by parallel studies on the biomineralization of calcium carbonate (calcite and aragonite) from amorphous calcium carbonate [52–54]. In the context of calcium phosphate biomineralization, calcium and phosphate ions are sequestered by biomimetic analogs of non-collagenous proteins involved in hard tissue mineralization into nanoparticles that exist in nanoscopical units known as prenucleation clusters [55–57]. These prenucleation clusters ($\approx$ 1 nm in diameter) eventually aggregate into larger (10–50 nm in diameter) liquid-like ACP nanoparticles. The latter, on penetration into the intrafibrillar water compartments of a collagen fibril, utilize the latter as a mineralization template, and undergo self-assembly and crystallographic alignment to form a metastable crystalline phase via mesoscale assembly. These mesocrystals probably fused to form iso-oriented crystal intermediates, and finally to single apatite crystallites within the 40 nm wide gap zone between the collagen molecules [23,58,59]. This ordered arrangement of apatite crystallites results in the manifestation of a banded appearance in unstained, mineralized fibrillar collagen [60].

2.2 Polymer-induced liquid precursor

Formation of amorphous nanoprecursors is the fundamental step in many forms of biomineralization. Existence of transient ACP nanoprecursors has been identified from enamel and bone [61–63]. In biomimetic mineralization of type I collagen, Dr. Gower and colleagues pioneered a process based on formation of a polymer-induced liquid- precursor (PILP) system [54,64]. The plasticity of liquid amorphous mineral precursors allows them to take the shape of their containers, resulting in a variety of biominerals with different hierarchical structures [65,66]. Using the PILP concept, Gower and colleagues were successful in mineralizing a variety of organic matrices with both calcium carbonate and calcium phosphate, including intrafibrillar mineralization of collagen matrices by carbonated apatite [47,67,68].

Based on the aforementioned new concepts of biomineralization introduced over the past decade, biomimetic mineralization of type I collagen may be envisaged to proceed in several stages [59]: 1) the collagen fibril serving as an active template for hierarchical intrafibrillar mineralization; 2) calcium and phosphate ions in the calcifying medium self-assemble into stable particulate units known as pre-nucleation clusters. In the presence of a polyanionic analog of matrix proteins such as poly(aspartic acid), these pre-nucleation clusters further condense into larger particles of fluidic amorphous ACP precursors (in the range of 10–30 nm) that are capable of diffusing into the intrafibrillar compartments of type I collagen; 3) the negatively charged polyanion-stabilized ACP precursors interact with positively-charged sites along the collagen molecules, inducing solidification and nucleation of the ACP inside collagen; 4) these nucleated amorphous mineral precursor phases further growth and

maturation into apatite nanocrystals along the intrafibrillar space of collagen via non-classical crystallization pathways; 5) Growth of the intrafibrillar apatite results in heavy intrafibrillar mineralization by apatite crystallites, with concomitant extrafibrillar mineralization between adjacent collagen fibrils.

2.3 Models of collagen mineralization

In our early studies, totally- or partially-demineralized dentin collagen matrices were employed for remineralization of hybrid layers and caries-like dentin lesions [17,20,28–36,69]. However, it is not known if the remineralization demonstrated in those studies was caused by the presence of remnant phosphoproteins that remain bound to collagen matrices after demineralization [70]. As self-assembled purified collagen fibrils do not contain bound matrix proteins, the authors employed a two-dimensional model of biomimetic mineralization of collagen based on reconstituted collagen fibrils deposited on grids used for transmission electron microscopy [71–73]. Briefly, bovine skin-derived type I collagen dissolved in acetic acid was reconstituted on formvar-coated grids by ammonia diffusion and cross-linked with 0.3 M carbodiimide. Then, the grid with a single layer of collagen was floated over a drop of a prospective biomimetic analog-containing biomineralization medium. The grid was retrieved at different time points (usually within 72 h) and rinsed with water. They were examined unstained for mineral deposition or stained for correlation of mineral deposition with collagen cross-striation patterns. With this model, we demonstrated a highly hierarchical assembly of intrafibrillar apatite crystallites in reconstituted collagen mineralized ex-situ with biomimetic analogs of extracellular matrix proteins [74] (Figure 1). This 2-D single-layer collagen mineralization model is useful as a rapid screening tool for potential biomimetic analogs for collagen mineralization [72]. Moreover, the technique may be modified for creating intrafibrillarly-mineralized collagen coatings on the surfaces of orthopedic and dental implants as a more bio-compatible alternative to the use of hydroxyapatite coatings [75].

Although the single-layer collagen model is a convenient and rapid method for studying biomimetic mineralization of individual collagen fibrils, the simple 2-D structure of the collagen model limits it further application. To further mimic natural collagen matrices, 3-D models of reconstituted collagen (Figure 2) were used by different research groups to evaluate the ability of the biomimetic mineralization scheme to mineralize collagen bundle assemblies within a three-dimensional scaffold [68,76]. Briefly, commercially available type I collagen sponges derived from bovine tendon were cultured in analog-containing biomineralization medium for 3–14 days. The mineralization assembly was kept in a 37°C oven to emulate physiological conditions. At predetermined reaction times, mineralized samples were removed from the solution, copiously washed with deionized water and further prepared for different analysis, including transmission electron microscopy, thermogravimetric analysis, attenuated total reflection-Fourier transform infrared spectroscopy, nuclear magnetic resonance spectroscopy and X-ray diffraction, which cannot be easily achieved with the 2-D collagen model [68,76,77]. The formed collagen–hydroxyapatite composites indicated that polyaspartic acid-stabilized ACP fluid droplets can diffuse into collagen bundles and mineralize a relatively thick collagen scaffold [77].

Although the mechanical properties of 3-D collagen sponges increase significantly after functional mineralization, they are still far less than those of the natural mineralized tissues because of their highly porous nature. Thus, attempts have been made by various groups to produce biomaterials that structurally mimic bone and dentin [68]. However, the hierarchical complexity of natural composites is usually far beyond contemporary bioengineering processing capability. One approach is to utilize the hierarchical structure of natural materials as a template for the development of high-performance engineering materials using in vitro biomimetic methods [78]. Thus, researchers revisited the use of natural

collagen model, including rat tail tendon (a soft tissue collagen 3D model; Figure 3), demineralized manatee bone and demineralized dentin collagen [68,79,80]. It was found that the amount of mineral present in the rat tail tendon samples represented the maximum amount of mineral available in the PILP solution [68]. Conversely, for demineralized manatee bone specimens, mineral distribution and penetration across the bulk of the bone matrix appears to be a challenge for the PILP process. The mineral penetration depth was limited to 100 μm [79]. The mineral content for the remineralized manatee bone specimens (about 45 wt%) was below the theoretical value for cortical bone, even though enough calcium and phosphate ions were available in the PILP solution to restore the mineral value of bone. It was proposed that auto-transformation and solidification of the surface-infiltrated ACP nanoprecursors into crystalline apatite with time could potentially block further infiltration of the additional nanoprecursors into the bulk of the demineralized bone matrix, thereby limiting their ultimate depth of penetration.

2.4 The need for using phosphate-containing biomimetic analogs in biomimetic mineralization of collagen

The functional role played by collagen in calcium phosphate biomineralization has been conjectural based on the results of the past several decades of research. Earlier studies indicated that fibrillar collagen does not initiate biomineralization on its own, but serves as a passive depot for the housing of apatite crystallites [70,81,82]. This led to a plethora of studies that examined the biological control of intrafibrillar collagen mineralization by noncollagenous proteins [83–88]. Noncollagenous proteins are believed to play a crucial role in the mineralization of bone and dentin. This assertion is supported by studies demonstrating that mutations in genes that code for these proteins result in abnormal bone and dentin mineralization [89–92]. The extracellular matrix of bone and dentin contains small quantities of noncollagenous proteins such as osteopontin, bone sialoprotein, dentin matrix protein 1 (DMP1), and dentin sialophosphoprotein (DSPP) [93,94]. The latter is further cleaved into dentin sialoprotein and dentin phosphoprotein (DPP; *aka* phosphophoryn) [95]. These proteins are highly anionic due to the prevalence of carboxylate groups on the polyaspartic acid residues that comprise the protein backbone. Post-translation phosphorylation of the serine residues produces phosphoserines, which further augments their anionic character [96,97]. For example, dentin phosphoprotein, being the most abundant NCP in dentin, contains a large number of aspartic acid (Asp) and phosphoserines (Pse) in the repeating sequences of $(Asp\text{-}Pse)_n$ and $(Asp\text{-}Pse\text{-}Pse)_n$ [98]. Dentin matrix protein 1, another member of the Small Integrin-Binding Ligand Interacting Glycoproteins (SIBLING) family, also contains high levels of Asp and Pse [99,100]. A unifying feature of the SIBLING proteins is that they all contain an Acidic Serine Aspartate-Rich MEPE (ASARM)-associated motif. The ASARM motif in SIBLING genes and the released ASARM peptide play roles in mineralization of bone and teeth [101,102]. The highly anionic nature of noncollagenous proteins involved in biomineralization enables them to sequester and bind calcium ions and presenting them to collagen fibrils at the mineralization front during the formation of bone and dentin.

In the authors' laboratory, biomimetic mineralization of collagen was performed using a dual biomimetic analog strategy [71–73,103–105]. Polyacrylic acid or polyaspartic acid was used as an analog for sequestering calcium ions released by set calcium silicate cements or a supersaturated calcium phosphate mineralization solution. These analogs function by acting as surfactants to prevent fluidic ACP nanoparticles from aggregating into larger particles, and to inhibit auto-transformation of the ACP nanoparticles into apatite (i.e. apatite nucleation inhibitor) prior to their entry into the intrafibrillar water compartments of the collagen fibril [71,72]. In addition, a polyphosphate-containing biomimetic analog such as polyvinylphosphonic acid, sodium trimetaphosphate or sodium ascorbyl phosphate was

employed as a templating biomimetic analog of matrix phosphoproteins. These phosphoprotein analogs were allowed to bind to the collagen fibrils prior to immersion of the fibrillar matrices in the poly(anionic) acid-containing mineralization medium [103–105]. Using the aforementioned collagen mineralization models, attachment of ACP nanoprecursors to the D-spacings of non-mineralized collagen fibrils was observed within 24 hours. After 48 hours, hierarchical apatite deposition was observed from unstained collagen fibrils that resulted in banded mineral arrangement. After 72 hours, highly-mineralized collagen fibrils could be seen in which the periodicity of the mineral arrangement was obscured as the fibrils were completely mineralized [71–74].

In contrast to the earlier work, more recent studies indicate that type I collagen plays an active role in biomineralization by acting as templates for physicochemical (electrostatic) attraction of ACP nanoparticles and direct formation of intrafibrillar apatite within the gap zones, without the intervention or mediation of other noncollagenous proteins present in vertebrate calcifying tissues [106,107]. Silver and Landis reported specific sites in the e2 band of the gap zones (corresponding to the a, e and d bands) of type I collagen that have the potential to sequester and bind calcium ions [108]. Nudelman *et al*. [58] calculated that there are net positive charges close to the C-terminal end of the collagen molecules that favor infiltration of the collagen fibrils with negatively charged ACP nanoprecursors. The arrangement of charged amino acids within the gap and overlap zones produce nucleation sites that control the conversion of the ACP nanoprecursors into oriented apatite crystals [58]. Indeed, several research groups have demonstrated that it is possible to produce intrafibrillar mineralization of type I collagen using poly(aspartic acid)-stabilized ACPs alone as an apatite nucleation inhibitor, without the adjunctive use of phosphorylated DDP, phosphorylated DMP1 or their polyphosphate analogs [58,79,109,110]. Although this simplified biomimetic collagen mineralization strategy is more economical and reduces time in preparing mineralized collagen scaffolds from a tissue engineering perspective, it begs the provision of a rationale for the existence of highly phosphorylated noncollagenous proteins in bone and dentin. The use of the simplified biomimetic mineralization strategy also challenges earlier biological studies that reported critical roles played by the phosphorylated forms of these noncollagenous proteins in the formation of mineralized collagenous tissues [96,99,111,112].

A recent study compared the effects of phosphorylated *vs* non-phosphorylated forms of DPP and DMP1 on collagen mineralization using a 2D model [113]. Although differences existed between DPP and DMP1 in the locations in which collagen fibrils were mineralized (intrafibrillar *vs* extrafibrillar), both phosphorylated proteins facilitated highly-organized intrafibrillar mineralization of collagen fibrils. Conversely, the use of non-phosphorylated forms of these proteins resulted in randomly-oriented intrafibrillar crystallites, with no particular organization of their crystallographic axes to the longitudinal axis of the collagen fibrils. Nevertheless, this study failed to explain why non-phosphorylated biomimetic apatite nucleation inhibitors such as polyaspartic acid or fetuin-A [114,115] are capable of producing highly-organized intrafibrillarly-mineralized collagen. It must be emphasized that while the concepts of particle-based ACP prenucleation clusters and the PILP phenomenon of fluidic ACP infiltration are new in collagen biomineralization research, the theoretical basis for interpretation of ultrastructural results of intrafibrillar apatite deposition is not [58,109], and is based upon the classic model of collagen molecular packing proposed by Petruska and Hodge [116]. This straight and rod-like model of steric arrangement of collagen molecules has since been replaced by a synchrotron X-ray diffraction-derived model in which collagen molecules are arranged in a right-handed helically-twisted, discontinuous manner along the length of the microfibrils [117]. In the latter model, interdigitation of adjacent microfibrils placed geometric constraints on the availability of

lateral intermolecular spacings between collagen molecules, with no room to accommodate apatite platelets outside the gap zones.

A recent study examined the effect of using single (polyacrylic acid) *vs* dual biomimetic analogs for mineralization of collagen fibrils (polyacrylic acid and sodium trimetaphosphate) [74]. In that study, polyacrylic acid was employed as an analog to inhibit apatite nucleation, and sodium trimetaphosphate was used as a templating analog for guiding intrafibrillar apatite deposition. The use of polyacrylic acid without a templating analog resulted only in intrafibrillar mineralization with continuous apatite strands. Conversely, the use of both analogs resulted in intrafibrillar mineralization with discrete apatite crystallites. While both methods resulted in intrafibrillar mineralization of collagen fibrils, the authors opined that in the absence of polyphosphate as a templating analog, infiltration of poly(anionic) acid-stabilized ACP nanoprecursors via a PILP process into the interconnecting water-filled volume within a collagen fibril appeared to have resulted in molding of ACP nanoprecursors into a continuum. This, in turn, resulted in crystallization of the carbonated apatite into a monolithic crystalline structure. Such a crystallization mechanism produces mineralized collagen entities that resemble the monolithic single-crystal structure in sea urchin spines or siliceous bio-skeletons. It is possible that release of poly(anionic) acid into the intrafibrillar milieu results in osmotic swelling and relaxation of the helical collagen microfibrillar arrangement, that facilitates continuous apatite deposition or growth from the gap zones into overlap zones into continuous strands. Conversely, electrostatic binding of polyphosphate analogs to discrete sites along the collagen molecules may have caused the bound analogs to act as inhibitor to discourage continuous growth of the apatite crystallites along the overlap zones, thereby resulting in constraining apatite platelets to the gap zones of the collagen fibril. This hypothesis is speculative and awaits further validation.

Nevertheless, the aforementioned hypothesis is consistent with the timely report comparing the ultrastructure of mineralized collagen in bone with the use of ion-milled sections *vs* sections prepared by conventional ultramicrotomy [118]. In ion-milled sections, the authors reported that approximately 70% of the minerals in bone are extrafibrillar, confirming previous models proposed by Lees *et al*. [119] and Hellmich and Ulm [120]. With respect to intrafibrillar apatite, crystallite platelets were only identified in the gap zones, without extension into the overlap zones, in contrast to what was previously proposed by Landis *et al*. [121]. Similar results were reported in another study using steric modeling to estimate the packing density of apatite within the gap zones [122]. Those modeling results were further confirmed using electron energy loss spectroscopy associated with scanning transmission electron microscopy. Taken together, these novel findings highlight that mechanisms in the control of discrete intrafibrillar apatite platelet deposition in the gap zones by phosphorylated NCPs are not completely understood. It is possible that the current success of intrafibrillar collagen mineralization with a single poly(anionic) acid analog may not result in truly biomimetically mineralized collagen that resembles those present in bone and dentin. These challenging issues require further in-depth investigations to decipher the riddles.

3 Adaptation of collagen biomineralization strategy for remineralization of resin-dentin bonds

Apart from increases in mechanical properties [123,124], a major role played by the presence of intrafibrillar apatite in mineralized collagen is the exclusion of molecules larger than water (*ca*. 18 Da) from the mineral-protein biocomposite [24]. Whereas even ethanol (*ca*. 46 Da) cannot solvate air-dried mineralized dentin, demineralized, water-filled collagen is susceptible to penetration by larger molecules. Molecules larger than 40 kDa are

completely excluded from the multiple internal water compartments [125] of type I collagen, while molecules smaller than 6 kDa can diffuse into all of the water compartments within the collagen fibril [126]. The physical exclusion of exogenous collagenolytic enzymes (bacterial collagenase − 68–130 kDa; activated MMP-2 − 67 kDa; activated MMP-9 – 85 kDa; activated cathepsin K – 27 kDa) by apatite forms the tenet of the “enzyme exclusion” mechanism that protects archeological collagen from degradation [127,128]. Experiments on collagenase hydrolysis of dentin have also confirmed the protective role played by the mineral phase on collagen degradation [129]. Endogenous MMPs and cysteine cathepsins, as well as other growth factors become “fossilized” by the intrafibrillar apatite minerals within dentin [130], but retain their biologic activities after they are incorporated into the mineralized dentin matrix. As collagen mineralizes, free and loosely-bound water is progressively replaced by apatite. This physiologic dehydration mechanism [131] ensures that the internal environment of the mineralized fibril remains relatively dry to preserve the integrity of the entrapped bioactive molecules [132].

In dentin bonding, the mineral phase of dentin is intentionally removed by acids, chelating agents or acidic resin monomers to expose the collagen for micromechanical retention of resins. As dentin demineralizes, bioactive molecules such as growth factors, matrix metalloproteinases and cysteine cathepsins are activated, provided that the demineralization agent is not strong enough to denature these molecules [3]. Contemporary etch-and-rinse and self-etch adhesives are incapable of completely replacing water from the extrafibrillar and intrafibrillar collagen compartments with resin monomers [21,133,134]. This can be seen by the number of publications on nanoleakage and micropermeability within hybrid layers. Biomimetic remineralization of resin-dentin bonds is a post-bonding technique that replaces intrafibrillar water as well as resin from water-rich, resin-sparse regions of the hybrid layer with intrafibrillar and extrafibrillar apatite crystallites [29]. By restoring the enzyme exclusion and fossilization properties of mineralized dentin, this proof-of-concept strategy is capable of preserving the longevity of resin-dentin bonds [35].

Both hybrid layers created by etch-and-rinse adhesives (Figure 4A) and those created by moderately aggressive (Figure 4B) and aggressive self-etching adhesives are amenable to the biomimetic remineralization approach. For etch-and-rinse adhesives, apatite crystallites can be detected in both extrafibrillar and intrafibrillar spaces after remineralization, as denuded collagen fibrils are present within those hybrid layers. Transmission electron microscopy of remineralized hybrid layers revealed that not the entire hybrid layer was remineralized [29,30]. Regions within hybrid layers that were well-infiltrated by adhesive resin monomers did not undergo remineralization. While the exact pattern of remineralization differed from specimen to specimen, the remineralized regions of poorly resin-infiltrated hybrid layers that (Figure 5A) in general corresponded well to water-rich, resin sparse regions of the hybrid layers that exhibited extensive silver nanoleakage when specimens were examined immediately after bonding (Figure 5B), or regions in which denuded collagen had been degraded after *in vivo* aging (Figure 5C). Along the surface of the hybrid layer, collagen fibrils that were unraveled due to the simultaneous action of cutting and phosphoric acid etching were remineralized in the form of continuous intrafibrillar strands, even when dual biomimetic analogs were employed (Figure 4C). This is possibly due to loosening of the microfibrillar arrangement and enlargement of the water compartments along the overlap zones of the collagen molecules, thereby enabling the ingress of poly(anionic) acid-stabilized ACP nanoprecursors into those regions. Conversely, collagen fibrils that were remineralized within the middle part of the hybrid layer contain discrete intrafibrillar apatite platelets (Figure 4D). These observations are in support of the hypothesis brought forward in Section 3.1 [74].

For self-etch adhesives, remineralization was not usually apparent in mild versions of these adhesives in which partially-demineralized dentin was present in the entire thickness of thin (< 0.5 μm thick) hybrid layers. Mild self-etch adhesives that contain the functional monomer 10-methacryloxydecyl dihydrogen phosphate (MDP) are capable of nano-layering with hydroxyapatite [135,136], thereby chemically interacting with the partially-demineralized apatite platelets to increase bond durability via the AD-concept [137]. For other mild self-etch adhesives that do not containing MDP, or those containing hydroxyethyl methacrylate that inhibit nanolayering of MDP [138], calcium phosphate deposition on remnant apatite platelets via epitaxial growth may have prevented the ultrastructural aspects of remineralization to be accurately depicted [22] without the use of a high resolution-transmission electron microscope. For moderately aggressive versions of self-etch adhesives, apatite deposition is almost exclusively identified from the completely-demineralized part of the hybrid layers. For the aggressive versions of self-etch adhesives, remineralization had been observed within the surface, middle or bottom parts of those thick hybrid layers, depending on the status of resin infiltration and the amount of water present within those hybrid layers. Apart from the use of transmission electron microscopy, the authors have employed a water-soluble fluorescent dye to backfill the water-rich regions within hybrid layers created by an aggressive self-etch adhesive and examined the dye-impregnated resin-dentin interface using confocal laser scanning microscopy [31,32]. In non-remineralized hybrid layers, water-rich regions within those hybrid layers and within the adhesive layer exhibit strong fluorescence of the dye. Interestingly, the intense fluorescence identified from those water-rich regions was quenched after biomimetic remineralization. These observations provide the evidence that biomimetic remineralization of hybrid layers is a process that progressively dehydrates water-rich hybrid layers. Unlike the conventional remineralization approach that proceeds rapidly via epitaxial growth over existing seed crystallites, biomimetic remineralization is a slower process as it involves at least two kinetically-driven pathways. Thus, it is important to prevent denuded collagen fibrils from degrading while they are being remineralized. Polyvinylphosphonic acid, a biomimetic analog used to simulate phosphorylated noncollagenous proteins, has been shown to possess matrix metalloproteinase-inhibiting properties that prevent collagen degradation during remineralization [139].

A critical problem encountered with the use of the other methods of matrix metalloproteinase and cysteine cathepsin inhibitors in extending the longevity of resin-dentin bonds is that hydrated, denuded collagen fibrils within the hybrid layer remain flaccid and exhibit weak mechanical properties even with preservation of their integrity [28]. The modulus of elasticity of resin-infiltrated dentin beams increased by 55–118% after biomimetic remineralization as a result of intrafibrillar mineralization of the collagen matrices [140]. A limitation of that study, however, is that the resin-infiltrated dentin beams (macro-hybrid layers) were evaluated *en mass*e using three-point bending. As remineralization does not occur in locations of the collagen matrices that are occupied by resins, three-point bending is insensitive in evaluating the localized increases in modulus of elasticity of the remineralized collagen fibrils. Due to the complexity of these regions, the authors have resorted to the use of nanoscopic dynamic mechanical analysis for characterizing the viscoplastic mechanical behavior of resin-infiltrated dentin before (Figure 6A) and after biomimetic remineralization (Figure 6B). This is achieved using scanning probe microscopy attached to a triboindentor to performed rasterized imaging and nanoindentations across an area of interest [141]. In addition, a method of scanning these hybrid layers under hydrated conditions was used to prevent water from evaporating from the specimens during scanning. This involves the application of a layer of ethylene glycol over the specimen surface to prevent water evaporation during a typical 25- to 30-min scanning period for a 25 × 25 μm area of the resin-dentin interface [36]. The combined use of nanoscopic dynamic mechanical analysis and scanning prove microscopy for mapping the

resin-dentin interface indicates that the complex modulus (E*), loss modulus (E") and storage modulus (E') of pre-aged hybrid layers created by an etch-and-rinse adhesive (E*, 3.86 ± 0.24; E″, 0.23 ± 0.05; E′, 3.85 ± 0.24 GPa) are much lower than those properties of the underlying mineralized dentin (E*, 19.20 ± 2.42; E″, 6.57 ± 1.96; E′, 17.39 ± 2.0 GPa). After aging of the resin-dentin bonds for 6 months, the water-rich, resin-sparse regions of the hybrid layers degraded, and the dynamic mechanical properties of those regions further declined (E*, 0.83 ± 0.35; E″, 0.88 ± 0.24; E′, 0.62 ± 0.32 GPa). Conversely, when aging of those bonds were performed concomitantly with biomimetic remineralization, those resin-sparse regions became remineralized by intrafibrillar and extrafibrillar apatite crystallites. The dynamic mechanical properties of those remineralized regions (E*, 19.73 ± 3.85; E″, 8.75 ± 3.97; E′, 16.02 ± 2.58 GPa) were restored to those values characteristic of intact mineralized dentin.

4 Biomimetic remineralization of carious dentin

Caries is a dynamic process caused by imbalance between demineralization and remineralization. Carious dentin can be classified into outer caries-infected dentin and inner caries-affected dentin [142]. Mineral distribution of caries-affected dentin is highly variable and the lesion depth can extend hundreds of micrometer below the excavated surface [143–146].Contemporary caries management is based on a conservative and preventive approach [147,148]. This minimum invasive philosophy avoids unnecessary tooth sacrifice and leaves caries-affected dentin as the clinical bonding substrate [149]. The bond strengths of dentin adhesives to caries-affected dentin substrate have been reported to be significantly lower than those bonded to noncarious dentin [150–153]. This is attributed to the obliteration of dentinal tubules by acid-resistant mineral crystals, a thicker zone of exposed collagen after the application of the adhesive and the lower stiffness and increased water content of the caries-affected dentin [154–158]. Unlike caries-infected dentin that is denatured, the collagen matrix of caries-affected dentin is not structurally and biochemically different from that found in sound dentin and is physiologically remineralizable [154,159,160].

Remineralization of partially-demineralized dentin is not new. Reports on remineralization of carious dentin appeared in the dental literature more than half a century ago. The dental literature also contains reports on the use of fluoride-releasing glass ionomer cements and calcium phosphate releasing dental materials [161–164] for remineralizing partially-demineralized carious dentin. Intact, non-denatured collagen is remineralizable as long as seed crystallites are present as niduses for heterogeneous nucleation of calcium phosphate phases [165]. Remineralization by epitaxial growth is a thermodynamically favorable process that overcomes the energy barriers of homogeneous nucleation [166]. In nanotechnology terminology, remineralization techniques currently employed in dentistry represent a top-down approach [167]. This approach creates materials using scaled down versions of a bulk material that incorporates nanoscale details of the original material. Partial demineralization of a mineralized collagen matrix by acids derived from bacteria or dentin bonding procedures creates the seed crystallites necessary for this top-down remineralization approach. The orientation of those remineralized crystalline lattices is pre-determined by the lattice of the original seed crystallites. However, remineralization does not occur in locations where seed crystallites are absent, as demonstrated with the use of a strontium-based glass ionomer cement on phosphoric acid-etched dentin [16]. This limitation severely restricts apatite-sparse superficial part of caries-affected dentin to be remineralized with a conventional top-down approach.

In biomineralization that occurs in nature, there are no seed crystallites present in an organic scaffold. Consequently, biomineralization has to proceed via an alternative pathway that involves homogeneous nucleation. One of the mechanisms of homogeneous nucleation

involves sequestration of amorphous mineral phase by polyanionic extracellular matrix protein molecules. Fluoride, which has been shown to enhance conventional remineralization via the top-down approach, is not employed by nature as a functional motif for biomineralization. In addition, fluoride-based dentin remineralization strategies also result in hypermineralization of the lesion surface [168,169] and prevent effective remineralization of the deeper parts of the carious lesion [170,171]. Homogeneous nucleation is not as thermodynamically favorable and involves alternative kinetically-driven protein/polymer-modulated pathways for lowering the activation energy barrier for crystal nucleation via sequential steps of phase transformations [18,172]. In nanotechnology terminology, such pathways are examples of a bottom-up approach [167], wherein nanoscale materials are created using a particle-based self-assembly process [37,47]

To evaluate the efficacy of a bottom-up approach to remineralize carious dentin, the authors created, via pH cycling, 250–300 μm thick artificial carious dentin lesions, each with a gradient of demineralization from the surface to the base of the lesion (Figure 7A) [17]. The artificial carious lesions were randomly divided into two groups and remineralized for 4 months using a classical top-down approach (Figure 7B) or a non-classical bottom-up approach (Figure 7C). In the bottom-up biomimetic remineralization strategy, two analogs were used to mimic the functions of matrix proteins in biomineralization. Polyacrylic was employed as an apatite nucleation inhibition agent to stabilize ACP nanoprecursors derived from set Portland cement or mineral trioxide aggregate (MTA) and simulated body fluid (SBF). Polyvinylphosphonic acid was used as a template to recruit the ACP nanoprecursors to the gap zones of the collagen fibrils, where they nucleate and self-assemble into hierarchically-arranged apatite nanocrystals within the gap zones of the collagen fibril. No analogs were used in the control top-down approach. To quantitatively assess the changes of mineral density before and after mineralization, micro-computed tomography was used to examine the mineralized collagen scaffold non-destructively in three dimensions, over a period of 4 months. To delineate between intrafibrillar and extrafibrillar apatite deposition within the collagen fibrils, transmission electron microscopy was used to examine the dimension and hierarchy of apatite deposition within the mineralized collagen matrix. It was found that the top-down approach could only mineralize the base of the partially-demineralized scaffold where remnant seed crystallites were abundant. Minimal mineralization was observed along the surface of the scaffold, wherein extrafibrillar mineralization was predominantly observed. Conversely, the entire partially-demineralized scaffold including apatite-depleted collagen fibrils was mineralized by the bottom-up approach, with evidence of both intrafibrillar and extrafibrillar mineralization. Similar results were obtained when polyvinylphosphonic acid was replaced by sodium trimetaphosphate as a biomimetic analog of phosphorylated noncollagen proteins to recruit polyacrylic acid-stabilized ACP nanoprecursors [33].

In a more recent study, Burwel *et al*. applied the PILP system (polyaspartic acid only as the apatite nucleation inhibition agent) to remineralize 140 μm deep artificial caries lesions for 7–28 days [80]. The authors examined the nanomechanical properties of the hydrated artificial lesions before remineralization and at different time points after biomimetic remineralization. Prior to remineralization, the hydrated artificial carious-like lesions had a low reduced elastic modulus of 0.2 GPa extending about 70 μm into the lesion, with a sloped region to about 140 μm where the reduced elastic modulus reached that in normal dentin (18–20 GPa). After 7 days of biomimetic remineralization, specimens recovered mechanical properties in the sloped region by 51% compared to the artificial lesion. Between 7–14 days, recovery of the outer portion of the lesion continued to a level of about 10 GPa with 74% improvement. After 28 days of PILP remineralization, there was 91% improvement of the reduced modulus compared to the artificial lesion. During remineralization, intrafibrillar mineral increased and crystallinity improved with intrafibrillar mineral exhibiting the

orientation found in normal dentin or bone. These researches generated important information to address the critical barrier to progress in remineralization of caries-affected dentin and shifted existing paradigms by providing a novel method of remineralization based on a nanotechnology-based bottom-up approach. All these results support the translation of the proof-of-concept biomimetic strategy into a clinically-relevant delivery system for remineralizing caries-affected dentin created by micro-organisms in the oral cavity.

5 From proof-of-concept to clinical translation – potential strategies

Although the particle-based biomimetic remineralization strategy based on the PILP process demonstrates great potential in remineralizing faulty hybrid layers or caries-like dentin, the strategy remains a proof-of-concept. To-date, studies published by various research groups utilized sectioned dentin slabs of the resin-dentin interface or artificially-created carious lesion and not the whole tooth for remineralization. These slabs were immersed in a metastable remineralization solution containing supersaturated calcium and phosphate ions, as well as the biomimetic analogs responsible for generating fluidic ACP nanoprecursors. Whereas poly(anionic acid)-stabilized ACP nanoprecursors can readily infiltrate sideways into the interfacial defect in a sectioned slab, this is not possible clinically. This is because the area occupied by the bonded dentin or carious dentin is segregated from the oral environment by a restorative material and only a very small part of the interface is exposed along the cavosurface margin. It is unrealistic for biomimetic remineralization to be accomplished through the use of a mouthrinse or a topically applied delivery system such as a remineralization paste or gel, wherein the polymer-stabilized-ACP nanoprecursors have to diffuse thousands of micrometers into the adhesive or caries-affected dentin within a restoration. For effective remineralization, the critical components of the biomimetic scheme (i.e. calcium and phosphate source and biomimetic analog/analogs) have to be incorporated into a dentin adhesive or restorative material. These critical components should be able to be released from polymerized resins. This necessitates incorporation of hydrophilic resin monomers in the adhesive or resin composite to facilitate water, ion and nanoparticulate diffusion. Although some calcium phosphate phases may precipitate within the adhesive or restorative material, it is critical that the bulk of the remineralization components diffuse through the adhesive joint to backfill water-rich regions of faulty hybrid layers or the caries-affected dentin with intrafibrillar apatite crystallites. To increase the durability of the restorations, there should also be sustained release of these critical components to remineralize tooth-restoration interfaces that have been subjected to secondary caries. These requirements impose considerable challenges to the translation of a scientifically-sound concept into a clinically-applicable approach, without adding extra steps into current bonding/restorative protocols.

The idea of incorporating calcium phosphate or bioactive glass particles into resins to develop composites with remineralizing capabilities has been explored by different researchers [14,15,173–178]. One group of composites contained ACP fillers, with the zirconia-stabilized ACP particles having a median diameter of 7.4 μm (ranging from 0.3 to 80 μm) [179]. However, in another study, the zirconia-stabilized ACP particles were larger, with a median diameter of 55 μm (ranging from submicron to 100 μm) [180]. These experimental calcium phosphate– containing composites are promising for remineralization of enamel because ACP is a precursor that forms initially and eventually transforms into apatite [181]. More recently, ACP nanoparticles with a much smaller diameter (116 nm) have been synthesized using a spray-drying technique [182]. Being solid nanoparticles that are used as fillers within a polymerized resin matrix, they are incapable of being released from the composite, or diffusing through the adhesive into faulty hybrid layers or adhesive-bonded caries-affected dentin [183]. Nevertheless, calcium and phosphate ions released

from these ACP nanoparticles can diffuse through water channels within the hydrophilic adhesive layer. Amorphous calcium phosphate nanoparticles have also been incorporated into experimental dentin adhesives [184,185]. In this case, the ACP nanoparticles are in closer proximity to the hybrid layer or caries-affected dentin. As the adhesive flows into dentinal tubules after the latter are rendered patent by acid-etching, incorporating ACP nanoparticles into a dentin adhesive may be more efficacious in remineralizing thick, partially-demineralized caries-affected dentin, as this shortens the path of diffusion of the calcium and phosphate ions, and reduces the chance of precipitation of calcium phosphate phases along the path of diffusion.

The use of ACP nanoparticle-containing dentin adhesive is innovative. These experimental adhesives are very likely to be able to remineralize partially-demineralized dentin by epitaxial deposition of calcium and phosphate phases over remnant apatite seed crystallites. However, the use of solid state ACP nanoparticles is not compliant with the non-classical theory of particle-based crystallization. Firstly, the ACP nanoparticles are still larger than the gap zone (40 nm) between the collagen molecules. Secondly, they do not possess the fluidic characteristics of amorphous mineral particles generated by a PILP process that enable them to infiltrate the intrafibrillar water compartments of collagen fibrils. Thirdly, although they release calcium and phosphate ions, they lack biomimetic analogs to sequester those ions into ACP prenucleation clusters. Thus, it is difficult to envisage how the use of preformed ACP nanoparticles can remineralize apatite-free denuded collagen fibrils within a faulty hybrid layer, or the superficial part of a caries lesion. It is pertinent to recapitulate that intrafibrillar mineralization of seed-crystallite free collagen is the hallmark of contemporary biomimetic collagen mineralization strategies. To date, intrafibrillar remineralization of dentin collagen has not been reported with the use of experimental adhesives containing solid ACP nanoparticles.

Another interesting form of stabilized ACP is casein phosphopeptide-ACP (CPP-ACP) [186]. Tryptic digestion of caseins derived from milk produces phosphopeptides that contain cluster of phosphoserine residues. The phosphorylated residues in CPP-ACP help to stabilize calcium and phosphate ions through the formation of complexes [187]. Theoretically, CPP can serve as a biomimetic analog of phosphorylated dentin noncollagenous proteins for recruiting ACP nanoprecursors into the gap zones of collagen fibrils. Although CPP-ACPs have been reported to be successful in the remineralization of non-cavitated demineralized enamel [188,189], evidence is lacking in terms of their ability to introduce intrafibrillar minerals into apatite-depleted dentin collagen fibrils.

A potential delivery strategy is to produce poly(anionic) acid-stabilized ACP prenucleation clusters and store them as “cargos” in mesoporous silica nanofillers (Figure 8). These mesoporous silica nanofillers may be incorporated in dentin adhesives as controlled release devices for the delivery of the ACP prenucleation clusters, or coalesced ACP fluidic PILP phases, into faulty hybrid layers or caries-affected dentin. The synthesis of mesoporous silica is based on the formation of liquid-crystalline mesophases of amphiphilic molecules (surfactants) that serve as templates for the *in-situ* polymerization of orthosilicic acid. The surfactants are then removed to produce nanoparticles with variable patterns of mesoporous channels. The mesoporous silica nanoparticles currently synthesized by the authors have a median particle diameter of 50 nm. They are composed of amorphous silica with a hexagonal system of mesopores, as determined by small angle X-ray diffraction. They have an extremely large specific surface area (>1000 m^2/g), as determined by nitrogen adsorption (Brunauer– Emmett–Teller method). This value is much higher than the specific surface area of the ACP nanoparticles (17.8 m^2/g) described previously [182]. The pore volume and pore size of the mesoporous silica nanoparticles synthesized in the authors’ laboratory, as determined by the Barrett-Joyner-Halenda method, is close to 1 cm^3/g and 3.5 nm,

respectively. As the average diameter of ACP prenucleation clusters 0.87±0.2 nm when they are first formed [55], they can readily enter the mesopores of the silica nanofillers. As the internal surface of the mesopores contains silanol groups that are negatively charged, different methods are available for functionalization of the internal pores to render them positively charged to enhance electrostatic attraction of the poly(anionic)acid-stabilized ACP nanoprecursors. The advantage of using mesoporous silica nanoparticles for delivery of ACP nanoprecursors is that silica is only sparingly soluble in an acidic environment. This prevents the silica nanoparticles and their loaded contents to be solubilized by acidic resin monomers present in some dentin adhesives. Another potential strategy currently contemplated by the authors is the use of calcium and phosphate-containing mesoporous bioactive glass nanoparticles synthesized by a sol-gel route for the loading and delivery of biomimetic analogs. The ion-releasing nanoparticles provide the source of calcium and phosphate for in-situ generation of prenucleation clusters. Research in the development of these novel nanotechnologies for clinical translation of the concept of biomimetic remineralization of dentin is in order.

Acknowledgments

This work was supported by grant R01 DE015306-06 from NIDCR (PI. David H Pashley), the ERA award and IRRM award from Georgia Regents University (PI. Franklin R Tay), National Nature Science Foundation of China grant 81130078 (PI. Jihua Chen), and National Key Basic Research Program of China grant 2012CB526704 (PI. Jihua Chen). We thank Michelle Burnside for secretarial support.

References

1. White DJ. The application of in vitro models to research on demineralization and remineralization of the teeth. Advances in Dental Research. 1995; 9:175–193. 94–7. [PubMed: 8615942]
2. Tersariol IL, Geraldeli S, Minciotti CL, Nascimento FD, Paakkonen V, Martins MT, et al. Cysteine cathepsins in human dentin-pulp complex. Journal of Endodontics. 2010; 36:475–481. [PubMed: 20171366]
3. Tjäderhane L, Nascimento FD, Breschi L, Mazzoni A, Tersariol IL, Geraldeli S, et al. Optimizing dentin bond durability: control of collagen degradation by matrix metalloproteinases and cysteine cathepsins. Dental Materials. 2013; 29:116–135. [PubMed: 22901826]
4. Bagramian RA, García-Godoy F, Volpe AR. The global increase in dental caries. A pending public health crisis. American Journal of Dentistry. 2009; 22:3–8. [PubMed: 19281105]
5. Loguercio AD, Moura SK, Pellizzaro A, Dal-Bianco K, Patzlaff RT, Grande RH, et al. Durability of enamel bonding using two-step self-etch systems on ground and unground enamel. Operative Dentistry. 2008; 33:79–88. [PubMed: 18335737]
6. De Munck J, Van Landuyt K, Peumans M, Poitevin A, Lambrechts P, Braem M, et al. A critical review of the durability of adhesion to tooth tissue: methods and results. Journal of Dental Research. 2005; 84:118–132. [PubMed: 15668328]
7. Liu Y, Tjäderhane L, Breschi L, Mazzoni A, Li N, Mao J, et al. Limitations in bonding to dentin and experimental strategies to prevent bond degradation. Journal of Dental Research. 2011; 90:953–968. [PubMed: 21220360]
8. Breschi L, Mazzoni A, Ruggeri A, Cadenaro M, Di Lenarda R, De Stefano DE. Dental adhesion review: aging and stability of the bonded interface. Dental Materials. 2008; 24:90–101. [PubMed: 17442386]
9. Sauro S, Watson TF, Mannocci F, Miyake K, Huffman BP, Tay FR, et al. Two-photon laser confocal microscopy of micropermeability of resin-dentin bonds made with water or ethanol wet bonding. Journal of Biomedical Materials Research B Applied Biomaterials. 2009; 90:327–337.
10. Carvalho RM, Manso AP, Geraldeli S, Tay FR, Pashley DH. Durability of bonds and clinical success of adhesive restorations. Dental Materials. 2012; 28:72–86. [PubMed: 22192252]

11. Bertassoni LE, Orgel JP, Antipova O, Swain MV. The dentin organic matrix - limitations of restorative dentistry hidden on the nanometer scale. Acta Biomaterialia. 2012; 8:2419–2433. [PubMed: 22414619]
12. Shen C, Zhang NZ, Anusavice KJ. Fluoride and chlorhexidine release from filled resins. Journal of Dental Research. 2010; 89:1002–1006. [PubMed: 20581354]
13. Xu HH, Moreau JL, Sun L, Chow LC. Nanocomposite containing amorphous calcium phosphate nanoparticles for caries inhibition. Dental Materials. 2011; 27:762–769. [PubMed: 21514655]
14. Sauro S, Osorio R, Watson TF, Toledano M. Therapeutic effects of novel resin bonding systems containing bioactive glasses on mineral-depleted areas within the bonded-dentine interface. Journal of Materials Science. Materials in Medicine. 2012; 23:1521–1532. [PubMed: 22466816]
15. Sauro S, Osorio R, Osorio E, Watson TF, Toledano M. Novel light-curable materials containing experimental bioactive micro-fillers remineralise mineral-depleted bonded-dentine interfaces. Journal of Biomaterials Science (Polymer Edition). 2013; 24:940–956.
16. Klont B, ten CJ. Remineralization of bovine incisor root lesions in vitro: the role of the collagenous matrix. Caries Research. 1991; 25:39–45. [PubMed: 2070381]
17. Kim YK, Yiu CK, Kim JR, Gu L, Kim SK, Weller RN, et al. Failure of a glass ionomer to remineralize apatite-depleted dentin. Journal of Dental Research. 2010; 89:230–235. [PubMed: 20110510]
18. Liu Y, Mai S, Li N, Yiu CK, Mao J, Pashley DH, et al. Differences between top-down and bottom-up approaches in mineralizing thick, partially demineralized collagen scaffolds. Acta Biomaterialia. 2011; 7:1742–1751. [PubMed: 21111071]
19. Nancollas G, Wu W. Biomineralization mechanisms: a kinetics and interfacial energy approach. Journal of Crystal Growth. 2000; 211:137–142.
20. Tay FR, Pashley DH. Guided tissue remineralisation of partially demineralised human dentine. Biomaterials. 2008; 29:1127–1137. [PubMed: 18022228]
21. Tay FR, Pashley DH. Biomimetic remineralization of resin-bonded acid-etched dentin. Journal of Dental Research. 2009; 88:719–724. [PubMed: 19734458]
22. Kim J, Arola DD, Gu L, Kim YK, Mai S, Liu Y, et al. Functional biomimetic analogs help remineralize apatite-depleted demineralized resin-infiltrated dentin via a bottom-up approach. Acta Biomaterialia. 2010; 6:2740–2750. [PubMed: 20045745]
23. Niederberger M, Cölfen H. Oriented attachment and mesocrystals: non-classical crystallization mechanisms based on nanoparticle assembly. Physical Chemistry Chemical Physics. 2006; 8:3271–3297. [PubMed: 16835675]
24. Cölfen, H.; Antonietti, M. Mesocrystals and Nonclassical Crystallization: New Self-assembled Structures. Hoboken, New Jersey: Wiley-Blackwell; 2008.
25. Lees S, Page EA. A study of some properties of mineralized turkey leg tendon. Connective Tissue Research. 1992; 28:263–287. [PubMed: 1304442]
26. Balooch M, Habelitz S, Kinney JH, Marshall SJ, Marshall GW. Mechanical properties of mineralized collagen fibrils as influenced by demineralization. Journal of Structural Biology. 2008; 162:404–410. [PubMed: 18467127]
27. Bertassoni LE, Habelitz S, Kinney JH, Marshall SJ, Marshall GW Jr. Biomechanical perspective on the remineralization of dentin. Caries Research. 2009; 43:70–77. [PubMed: 19208991]
28. Bertassoni LE, Habelitz S, Marshall SJ, Marshall GW. Mechanical recovery of dentin following remineralization in vitro--an indentation study. Journal of Biomechanics. 2011; 44:176–181. [PubMed: 20926080]
29. Mai S, Kim YK, Toledano M, Breschi L, Ling JQ, Pashley DH, et al. Phosphoric acid esters cannot replace polyvinylphosphonic acid as phosphoprotein analogs in biomimetic remineralization of resin-bonded dentin. Dental Materials. 2009; 25:1230–1239. [PubMed: 19481792]
30. Mai S, Kim YK, Kim J, Yiu CK, Ling J, Pashley DH, et al. In vitro remineralization of severely compromised bonded dentin. Journal of Dental Research. 2010; 89:405–410. [PubMed: 20173183]
31. Kim J, Vaughn RM, Gu L, Rockman RA, Arola DD, Schafer TE, et al. Imperfect hybrid layers created by an aggressive one-step self-etch adhesive in primary dentin are amendable to biomimetic remineralization in vitro. Journal of Biomedical Materials Research A. 2010; 93:1225–1234.

32. Kim J, Mai S, Carrilho MR, Yiu CK, Pashley DH, Tay FR. An all-in-one adhesive does not etch beyond hybrid layers. Journal of Dental Research. 2010; 89:482–487. [PubMed: 20200420]
33. Liu Y, Li N, Qi Y, Niu LN, Elshafiy S, Mao J, et al. The use of sodium trimetaphosphate as a biomimetic analog of matrix phosphoproteins for remineralization of artificial caries-like dentin. Dental Materials. 2011; 27:465–477. [PubMed: 21354608]
34. Qi YP, Li N, Niu LN, Primus CM, Ling JQ, Pashley DH, et al. Remineralization of artificial dentinal caries lesions by biomimetically modified mineral trioxide aggregate. Acta Biomaterialia. 2012; 8:836–842. [PubMed: 22085925]
35. Kim YK, Mai S, Mazzoni A, Liu Y, Tezvergil-Mutluay A, Takahashi K, et al. Biomimetic remineralization as a progressive dehydration mechanism of collagen matrices--implications in the aging of resin-dentin bonds. Acta Biomaterialia. 2010; 6:3729–3739. [PubMed: 20304110]
36. Ryou H, Niu LN, Dai L, Pucci CR, Arola DD, Pashley DH, et al. Effect of biomimetic remineralization on the dynamic nanomechanical properties of dentin hybrid layers. Journal of Dental Research. 2011; 90:1122–1128. [PubMed: 21730254]
37. Xu A, Ma Y, Cölfen H. Biomimetic mineralization. Journal of Materials Chemistry. 2007; 17:415–449.
38. Baeuerlein, E. Handbook of biomineralization. Volume I: biological aspects and structure formation. Weinheim: Wiley-VCH; 2007.
39. Veis A. Mineral-matrix interactions in bone and dentin. Journal of Bone and Mineral Research. 1993; 8(Suppl 2):493–497.
40. Boskey AL. Biomineralization: conflicts, challenges, and opportunities. Journal of Cell Biochemistry (Supplement). 1998; 30–31:83–91.
41. Hunter GK, Hauschka PV, Poole AR, Rosenberg LC, Goldberg HA. Nucleation and inhibition of hydroxyapatite formation by mineralized tissue proteins. Biochemical Journal. 1996; 317(Pt):59–64. [PubMed: 8694787]
42. Gajjeraman S, Narayanan K, Hao J, Qin C, George A. Matrix macromolecules in hard tissues control the nucleation and hierarchical assembly of hydroxyapatite. The Journal of Biological Chemistry. 2007; 282:1193–1204. [PubMed: 17052984]
43. Qin C, D'Souza R, Feng JQ. Dentin matrix protein 1 (DMP1): new and important roles for biomineralization and phosphate homeostasis. Journal of Dental Research. 2007; 86:1134–1141. [PubMed: 18037646]
44. Goldberg HA, Warner KJ, Li MC, Hunter GK. Binding of bone sialoprotein, osteopontin and synthetic polypeptides to hydroxyapatite. Connective Tissue Research. 2001; 42:25–37. [PubMed: 11696986]
45. Wang Y, Yang C, Chen X, Zhao N. Biomimetic formation of hydroxyapatite/collagen matrix composite. Advanced Engineering Materials. 2006; 8:97–100.
46. Li X, Chang J. Preparation of bone-like apatite-collagen nanocomposites by a biomimetic process with phosphorylated collagen. Journal of Biomedical Materials Research A. 2008; 85:293–300.
47. Gower LB. Biomimetic model systems for investigating the amorphous precursor pathway and its role in biomineralization. Chemistry Review. 2008; 108:4551–4627.
48. Sears RP. The non-classical nucleation of crystals: microscopic mechanisms and applications to molecular crystals, ice and calcium carbonate. International Materials Review. 2012; 57:328–356.
49. Traub W, Arad T, Weiner S. Origin of mineral crystal growth in collagen fibrils. Matrix. 1992; 12:251–255. [PubMed: 1435508]
50. Cölfen H, Mann S. Higher-order organization by mesoscale self-assembly and transformation of hybrid nanostructures. Angewandte Chemie International Edition (English). 2003; 42:2350–2365.
51. Fang J, Ding B, Gleiter H. Mesocrystals: syntheses in metals and applications. Chemical Society Reviews. 2011; 40:5347–5360. [PubMed: 21769374]
52. Kulak AN, Iddon P, Li Y, Armes SP, Cölfen H, Paris O, et al. Continuous structural evolution of calcium carbonate particles: a unifying model of copolymer-mediated crystallization. Journal of the American Chemical Society. 2007; 129:3729–3736. [PubMed: 17335283]
53. Seto J, Ma Y, Davis SA, Meldrum F, Gourrier A, Kim YY, et al. Structure-property relationships of a biological mesocrystal in the adult sea urchin spine. Proceedings of the National Academy of Science U S A. 2012; 109:3699–3704.

54. Olszta MJ, Odom DJ, Douglas EP, Gower LB. A new paradigm for biomineral formation: mineralization via an amorphous liquid-phase precursor. Connective Tissue Research. 2003; 44(Suppl 1):326–334. [PubMed: 12952217]
55. Dey A, Bomans PH, Muller FA, Will J, Frederik PM, de With G, et al. The role of prenucleation clusters in surface-induced calcium phosphate crystallization. Nature Materials. 2010; 9:1010–1014.
56. Gebauer D, Cölfen H. Prenucleation clusters and non-classical nucleation. Nano Today. 2011; 6:564–584.
57. Du LW, Bian S, Gou BD, Jiang Y, Huang J, Gao YX, et al. Structure of clusters and formation of amorphous calcium phosphate and hydroxyapatite: From the perspective of coordination chemistry. Crystal Growth & Design. 2013 in press.
58. Nudelman F, Pieterse K, George A, Bomans PH, Friedrich H, Brylka LJ, et al. The role of collagen in bone apatite formation in the presence of hydroxyapatite nucleation inhibitors. Nature Materials. 2010; 9:1004–1009.
59. Cölfen H. Biomineralization: A crystal-clear view. Nature Materials. 2010; 9:960–961.
60. Landis WJ. The strength of a calcified tissue depends in part on the molecular structure and organization of its constituent mineral crystals in their organic matrix. Bone. 1995; 16:533–544. [PubMed: 7654469]
61. Crane NJ, Popescu V, Morris MD, Steenhuis P Jr. Ignelzi MA. Raman spectroscopic evidence for octacalcium phosphate and other transient mineral species deposited during intramembranous mineralization. Bone. 2006; 39:434–442. [PubMed: 16627026]
62. Mahamid J, Sharir A, Addadi L, Weiner S. Amorphous calcium phosphate is a major component of the forming fin bones of zebrafish: Indications for an amorphous precursor phase. Proceedings of the National Academy of Science U S A. 2008; 105:12748–12753.
63. Beniash E, Metzler RA, Lam RS, Gilbert PU. Transient amorphous calcium phosphate in forming enamel. Journal of Structural Biology. 2009; 166:133–143. [PubMed: 19217943]
64. Olszta MJ, Douglas EP, Gower LB. Scanning electron microscopic analysis of the mineralization of type I collagen via a polymer-induced liquid-precursor (PILP) process. Calcified Tissue International. 2003; 72:583–591. [PubMed: 12616327]
65. Cheng X, Gower LB. Molding mineral within microporous hydrogels by a polymer-induced liquid-precursor (PILP) process. Biotechnology Progress. 2006; 22:141–149. [PubMed: 16454504]
66. Meldrum FC, Ludwigs S. Template-directed control of crystal morphologies. Macromolecular Bioscience. 2007; 7:152–162. [PubMed: 17295402]
67. Kim YY, Douglas EP, Gower LB. Patterning inorganic ($CaCO_3$) thin films via a polymer-induced liquid-precursor process. Langmuir. 2007; 23:4862–4870. [PubMed: 17388609]
68. Thula TT, Svedlund F, Rodriguez DE, Podschun J, Pendi L, Gower LB. Mimicking the nanostructure of bone: Comparison of polymeric process-directing agents. Polymers (Basel). 2011; 3:10–35. [PubMed: 22328971]
69. Tay FR, Pashley DH. Guided tissue remineralisation of partially demineralised human dentine. Biomaterials. 2008; 29:1127–1137. [PubMed: 18022228]
70. Saito T, Yamauchi M, Crenshaw MA. Apatite induction by insoluble dentin collagen. Journal of Bone and Mineral Research. 1998; 13:265–270. [PubMed: 9495520]
71. Kim YK, Gu LS, Bryan TE, Kim JR, Chen L, Liu Y, et al. Mineralisation of reconstituted collagen using polyvinylphosphonic acid/polyacrylic acid templating matrix protein analogues in the presence of calcium, phosphate and hydroxyl ions. Biomaterials. 2010; 31:6618–6627. [PubMed: 20621767]
72. Liu Y, Li N, Qi YP, Dai L, Bryan TE, Mao J, et al. Intrafibrillar collagen mineralization produced by biomimetic hierarchical nanoapatite assembly. Advanced Materials. 2011; 23:975–980. [PubMed: 21341310]
73. Dai L, Qi YP, Niu LN, Liu Y, Pucci CR, Looney SW, et al. Inorganic-organic nanocomposite assembly using collagen as template and sodium tripolyphosphate as a biomimetic analog of matrix phosphoprotein. Crystal Growth & Design. 2011; 11:3504–3511. [PubMed: 21857797]
74. Liu Y, Kim YK, Dai L, Li N, Khan SO, Pashley DH, et al. Hierarchical and non-hierarchical mineralisation of collagen. Biomaterials. 2011; 32:1291–1300. [PubMed: 21040969]

75. de Jonge LT, Leeuwenburgh SC, van den Beucken JJ, te RJ, Daamen WF, Wolke JG, et al. The osteogenic effect of electrosprayed nanoscale collagen/calcium phosphate coatings on titanium. Biomaterials. 2010; 31:2461–2469. [PubMed: 20022365]
76. Jee SS, Thula TT, Gower LB. Development of bone-like composites via the polymerinduced liquid-precursor (PILP) process.Part 1: influence of polymer molecular weight. Acta Biomaterialia. 2010; 6:3676–3686. [PubMed: 20359554]
77. Li Y, Thula TT, Jee S, Perkins SL, Aparicio C, Douglas EP, et al. Biomimetic mineralization of woven bone-like nanocomposites: role of collagen cross-links. Biomacromolecules. 2012; 13:49–59. [PubMed: 22133238]
78. George A, Ravindran S. Protein templates in hard tissue engineering. Nano Today. 2010; 5:254–266. [PubMed: 20802848]
79. Thula TT, Rodriguez DE, Lee MH, Pendi L, Podschun J, Gower LB. In vitro mineralization of dense collagen substrates: a biomimetic approach toward the development of bone-graft materials. Acta Biomaterialia. 2011; 7:3158–3169. [PubMed: 21550424]
80. Burwell AK, Thula-Mata T, Gower LB, Habeliz S, Kurylo M, Ho SP, et al. Functional remineralization of dentin lesions using polymer-induced liquid-precursor process. PLoS One. 2012; 7:e38852. [PubMed: 22719965]
81. Glimcher MJ. Mechanism of calcification: role of collagen fibrils and collagen-phosphoprotein complexes in vitro and in vivo. The Anatomical Record. 1989; 224:139–153. [PubMed: 2672881]
82. Glimcher MJ. The possible role of collagen fibrils and collagen-phosphoprotein complexes in the calcification of bone in vitro and in vivo. Biomaterials. 1990; 11:7–10. [PubMed: 2204439]
83. Hunter GK, Kyle CL, Goldberg HA. Modulation of crystal formation by bone phosphoproteins: structural specificity of the osteopontin-mediated inhibition of hydroxyapatite formation. Biochemical Journal. 1994; 300(Pt 3):723–728. [PubMed: 8010953]
84. Hunter GK, Hauschka PV, Poole AR, Rosenberg LC, Goldberg HA. Nucleation and inhibition of hydroxyapatite formation by mineralized tissue proteins. Biochemical Journal. 1996; 317(Pt 1): 59–64. [PubMed: 8694787]
85. Saito T, Yamauchi M, Abiko Y, Matsuda K, Crenshaw MA. In vitro apatite induction by phosphophoryn immobilized on modified collagen fibrils. Journal of Bone and Mineral Research. 2000; 15:1615–1619. [PubMed: 10934661]
86. Tye CE, Rattray KR, Warner KJ, Gordon JA, Sodek J, Hunter GK, et al. Delineation of the hydroxyapatite-nucleating domains of bone sialoprotein. The Journal of Biological Chemistry. 2003; 278:7949–7955. [PubMed: 12493752]
87. Baht GS, Hunter GK, Goldberg HA. Bone sialoprotein-collagen interaction promotes hydroxyapatite nucleation. Matrix Biology. 2008; 27:600–608. [PubMed: 18620053]
88. de Bruyn JR, Goiko M, Mozaffari M, Bator D, Dauphinee RL, Liao Y, et al. Dynamic light scattering study of inhibition of nucleation and growth of hydroxyapatite crystals by osteopontin. PLoS One. 2013; 8:e56764. [PubMed: 23457612]
89. Sreenath T, Thyagarajan T, Hall B, Longenecker G, D'Souza R, Hong S, et al. Dentin sialophosphoprotein knockout mouse teeth display widened predentin zone and develop defective dentin mineralization similar to human dentinogenesis imperfecta type III. The Journal of Biological Chemistry. 2003; 278:24874–24880. [PubMed: 12721295]
90. Dong J, Gu T, Jeffords L, MacDougall M. Dentin phosphoprotein compound mutation in dentin sialophosphoprotein causes dentinogenesis imperfecta type III. American Journal of Medical Genetics Part A. 2005; 132A:305–309. [PubMed: 15690376]
91. Sun Y, Chen L, Ma S, Zhou J, Zhang H, Feng JQ, et al. Roles of DMP1 processing in osteogenesis, dentinogenesis and chondrogenesis. Cells Tissues Organs. 2011; 194:199–204. [PubMed: 21555863]
92. Sun Y, Lu Y, Chen L, Gao T, D'Souza R, Feng JQ, et al. DMP1 processing is essential to dentin and jaw formation. Journal Of Dental Research. 2011; 90:619–624. [PubMed: 21297011]
93. Veis A. Mineral-matrix interactions in bone and dentin. Journal of Bone and Mineral Research. 1993; 8:493–497.Suppl 2
94. Boskey AL. Biomineralization: conflicts, challenges, and opportunities. Journal of Cell Biochemistry (Supplement). 1998; 30–31:83–91.

95. MacDougall M, Simmons D, Luan X, Nydegger J, Feng J, Gu TT. Dentin phosphoprotein and dentin sialoprotein are cleavage products expressed from a single transcript coded by a gene on human chromosome 4. Dentin phosphoprotein DNA sequence determination. The Journal of Biological Chemistry. 1997; 272:835–842. [PubMed: 8995371]

96. Veis A, Sfeir C, Wu CB. Phosphorylation of the proteins of the extracellular matrix of mineralized tissues by casein kinase-like activity. Critical Review in Oral Biology & Medicine Med. 1997; 8:360–379.

97. Qin C, Baba O, Butler WT. Post-translational modifications of sibling proteins and their roles in osteogenesis and dentinogenesis. Critical Review in Oral Biology & Medicine. 2004; 15:126–136.

98. Prasad M, Butler WT, Qin C. Dentin sialophosphoprotein in biomineralization. Connective Tissue Research. 2010; 51:404–417. [PubMed: 20367116]

99. He G, Gajjeraman S, Schultz D, Cookson D, Qin C, Butler WT, et al. Spatially and temporally controlled biomineralization is facilitated by interaction between self-assembled dentin matrix protein 1 and calcium phosphate nuclei in solution. Biochemistry. 2005; 44:16140–16148. [PubMed: 16331974]

100. Fisher LW. DMP1 and DSPP: evidence for duplication and convergent evolution of two SIBLING proteins. Cells Tissues Organs. 2011; 194:113–118. [PubMed: 21555860]

101. Boskey AL, Chiang P, Fermanis A, Brown J, Taleb H, David V, et al. MEPE's diverse effects on mineralization. Calcified Tissue International. 2010; 86:42–46. [PubMed: 19998030]

102. Rowe PS. Regulation of bone-renal mineral and energy metabolism: the PHEX, FGF23, DMP1, MEPE ASARM pathway. Critical Reviews in Eukaryotic Gene Expression. 2012; 22:61–86. [PubMed: 22339660]

103. Gu LS, Kim J, Kim YK, Liu Y, Dickens SH, Pashley DH, et al. A chemical phosphorylation-inspired design for type I collagen biomimetic remineralization. Dental Materials. 2010; 26:1077–1089. [PubMed: 20688381]

104. Gu LS, Kim YK, Liu Y, Takahashi K, Arun S, Wimmer CE, et al. Immobilization of a phosphonated analog of matrix phosphoproteins within cross-linked collagen as a templating mechanism for biomimetic mineralization. Acta Biomaterialia. 2011; 7:268–277. [PubMed: 20688200]

105. Gu L, Kim YK, Liu Y, Ryou H, Wimmer CE, Dai L, et al. Biomimetic analogs for collagen biomineralization. Journal of Dental Research. 2011; 90:82–87. [PubMed: 20940362]

106. Wang Y, Azais T, Robin M, Vallee A, Catania C, Legriel P, et al. The predominant role of collagen in the nucleation, growth, structure and orientation of bone apatite. Nature Materials. 2012; 11:724–733.

107. Landis W, Silver F, Freeman J. Collagen as a scaffold for biomimetic mineralization of vertebrate tissues. Journal of Materials Chemistry. 2006; 16:1495–1503.

108. Silver FH, Landis WJ. Deposition of apatite in mineralizing vertebrate extracellular matrices: A model of possible nucleation sites on type I collagen. Connective Tissue Research. 2011; 52:242–254. [PubMed: 21405976]

109. Olszta M, Cheng X, Jee S, Kumar R, Kim Y, Kaufman M, et al. Bone structure and formation: A new perspective. Materials Science and Engineering R. 2007; 558:77–116.

110. Deshpande AS, Beniash E. Bio-inspired synthesis of mineralized collagen fibrils. Crystal Growth & Design. 2008; 8:3084–3090. [PubMed: 19662103]

111. He G, Ramachandran A, Dahl T, George S, Schultz D, Cookson D, et al. Phosphorylation of phosphophoryn is crucial for its function as a mediator of biomineralization. The Journal of Biological Chemistry. 2005; 280:33109–33114. [PubMed: 16046405]

112. George A, Veis A. Phosphorylated proteins and control over apatite nucleation, crystal growth, and inhibition. Chemical Reviews. 2008; 108:4670–4693. [PubMed: 18831570]

113. Deshpande AS, Fang PA, Zhang X, Jayaraman T, Sfeir C, Beniash E. Primary structure and phosphorylation of dentin matrix protein 1 (DMP1) and dentin phosphophoryn (DPP) uniquely determine their role in biomineralization. Biomacromolecules. 2011; 12:2933–2945. [PubMed: 21736373]

114. Schinke T, Amendt C, Trindl A, Poschke O, Muller-Esterl W, Jahnen-Dechent W. The serum protein alpha2-HS glycoprotein/fetuin inhibits apatite formation in vitro and in mineralizing

calvaria cells. A possible role in mineralization and calcium homeostasis. The Journal of Biological Chemistry. 1996; 271:20789–20796. [PubMed: 8702833]

115. Price PA, Toroian D, Lim JE. Mineralization by inhibitor exclusion: the calcification of collagen with fetuin. The Journal of Biological Chemistry. 2009; 284:17092–17101. [PubMed: 19414589]
116. Petruska J, Hodge A. A subunit model for the tropocollagen macromolecule. Proceedings of the National Academy of Science U S A. 1964; 51:871–876.
117. Orgel JP, Irving TC, Miller A, Wess TJ. Microfibrillar structure of type I collagen in situ. Proceedings of the National Academy of Science U S A. 2006; 103:9001–9005.
118. McNally EA, Schwarcz HP, Botton GA, Arsenault AL. A model for the ultrastructure of bone based on electron microscopy of ion-milled sections. PLoS One. 2012; 7:e29258. [PubMed: 22272230]
119. Lees S, Prostak KS, Ingle VK, Kjoller K. The loci of mineral in turkey leg tendon as seen by atomic force microscope and electron microscopy. Calcified Tissue International. 1994; 55:180–189. [PubMed: 7987731]
120. Hellmich C, Ulm FJ. Average hydroxyapatite concentration is uniform in the extracollagenous ultrastructure of mineralized tissues: evidence at the 1-10-microm scale. tBiomechanics and Modeling in Mechanobiology. 2003; 2:21–36.
121. Landis WJ, Hodgens KJ, Arena J, Song MJ, McEwen BF. Structural relations between collagen and mineral in bone as determined by high voltage electron microscopic tomography. Microscopy Research and Techique. 1996; 33:192–202.
122. Alexander B, Daulton TL, Genin GM, Lipner J, Pasteris JD, Wopenka B, et al. The nanometre-scale physiology of bone: steric modelling and scanning transmission electron microscopy of collagen-mineral structure. Journal of the Royal Society Interface. 2012; 9:1774–1786.
123. Kinney JH, Habelitz S, Marshall SJ, Marshall GW. The importance of intrafibrillar mineralization of collagen on the mechanical properties of dentin. Journal of Dental Research. 2003; 82:957–961. [PubMed: 14630894]
124. Balooch M, Habelitz S, Kinney JH, Marshall SJ, Marshall GW. Mechanical properties of mineralized collagen fibrils as influenced by demineralization. Journal of Structural Biology. 2008; 162:404–410. [PubMed: 18467127]
125. Cameron IL, Short NJ, Fullerton GD. Verification of simple hydration/dehydration methods to characterize multiple water compartments on tendon type 1 collagen. Cell Biology International. 2007; 31:531–539. [PubMed: 17363297]
126. Toroian D, Lim JE, Price PA. The size exclusion characteristics of type I collagen: implications for the role of noncollagenous bone constituents in mineralization. The Journal of Biological Chemistry. 2007; 282:22437–22447. [PubMed: 17562713]
127. Nielsen-Marsh CM, Hedges REM, Mann T, Collins MJ. A preliminary investigation of the application of differential scanning calorimetry to the study of collagen degradation in archaeological bone. Thermochimica Acta. 2000; 365:129–139.
128. Collins MJ, Nielsen-Marsh CM, Hiller J, Smith CJ, Roberts JP, Progodich RV, et al. The survival of organic matter in bone: a review. Archaeometry. 2002; 44:383–394.
129. Osorio R, Yamauti M, Sauro S, Watson TF, Toledano M. Experimental resin cements containing bioactive fillers reduce matrix metalloproteinase-mediated dentin collagen degradation. Journal of Endodontics. 2012; 38:1227–1232. [PubMed: 22892740]
130. Smith AJ. Vitality of the dentin-pulp complex in health and disease: growth factors as key mediators. Journal of Dental Education. 2003; 67:678–689. [PubMed: 12856968]
131. Chesnick IE, Mason JT, Giuseppetti AA, Eidelman N, Potter K. Magnetic resonance microscopy of collagen mineralization. Biophysical Journal. 2008; 95:2017–2026. [PubMed: 18487295]
132. Wehrli FW, Fernández-Seara MA. Nuclear magnetic resonance studies of bone water. Ann Biomed Eng. 2005; 33:79–86. [PubMed: 15709708]
133. Brackett MG, Li N, Brackett WW, Sword RJ, Qi YP, Niu LN, et al. The critical barrier to progress in dentine bonding with the etch-and-rinse technique. Journal of Dentistry. 2011; 39:238–248. [PubMed: 21215788]

134. Kim J, Gu L, Breschi L, Tjäderhane L, Choi KK, Pashley DH, Tay FR. Implication of ethanol wet-bonding in hybrid layer remineralization. Journal of Dental Research. 2010; 89:575–580. [PubMed: 20200419]

135. Yoshihara K, Yoshida Y, Hayakawa S, Nagaoka N, Irie M, Ogawa T, et al. Nanolayering of phosphoric acid ester monomer on enamel and dentin. Acta Biomaterialia. 2011; 7:3187–3195. [PubMed: 21575747]

136. Yoshida Y, Yoshihara K, Nagaoka N, Hayakawa S, Torii Y, Ogawa T, et al. Self-assembled nano-layering at the adhesive interface. Journal of Dental Research. 2012; 91:376–381. [PubMed: 22302145]

137. Van Meerbeek B, Yoshihara K, Yoshida Y, Mine A, De Munck J, Van Landuyt KL. State of the art of self-etch adhesives. Dental Materials. 2011; 27:17–28. [PubMed: 21109301]

138. Yoshida Y, Yoshihara K, Hayakawa S, Nagaoka N, Okihara T, Matsumoto T, et al. HEMA inhibits interfacial nano-layering of the functional monomer MDP. Journal of Dental Research. 2012; 91:1060–1065. [PubMed: 22968157]

139. Tezvergil-Mutluay A, Agee KA, Hoshika T, Tay FR, Pashley DH. The inhibitory effect of polyvinylphosphonic acid on functional matrix metalloproteinase activities in human demineralized dentin. Acta Biomaterialia. 2010; 6:4136–4142. [PubMed: 20580949]

140. Gu LS, Huffman BP, Arola DD, Kim YK, Mai S, Elsalanty ME, et al. Changes in stiffness of resin-infiltrated demineralized dentin after remineralization by a bottom-up biomimetic approach. Acta Biomaterialia. 2010; 6:1453–1461. [PubMed: 19887126]

141. Ryou H, Pashley DH, Tay FR, Arola D. A characterization of the mechanical behavior of resin-infiltrated dentin using nanoscopic Dynamic Mechanical Analysis. Dental Materials. 2013 [Epub ahead of print].

142. Fusayama T, Terachima S. Differentiation of two layers of carious dentin by staining. Journal of Dental Research. 1972; 51:866. [PubMed: 4113394]

143. Ogushi K, Fusayama T. Electron microscopic structure of the two layers of carious dentin. Journal of Dental Research. 1975; 54:1019–1026. [PubMed: 1058852]

144. Zavgorodniy AV, Rohanizadeh R, Swain MV. Ultrastructure of dentine carious lesions. Archives of Oral Biology. 2008; 53:124–132. [PubMed: 17915189]

145. Pugach MK, Strother J, Darling CL, Fried D, Gansky SA, Marshall SJ, et al. Dentin caries zones: mineral, structure, and properties. Journal of Dental Research. 2009; 88:71–76. [PubMed: 19131321]

146. Almahdy A, Downey FC, Sauro S, Cook RJ, Sherriff M, et al. Microbiochemical analysis of carious dentine using Raman and fluorescence spectroscopy. Caries Research. 2012; 46:432–440. [PubMed: 22739587]

147. Thompson V, Craig RG, Curro FA, Green WS, Ship JA. Treatment of deep carious lesions by complete excavation or partial removal: a critical review. Journal of the American Dental Association. 2008; 139:705–712. [PubMed: 18519994]

148. Kidd EA. Clinical threshold for carious tissue removal. Dental Clinics of North America. 2010; 54:541–549. [PubMed: 20630195]

149. Fusayama T. Two layers of carious dentin; diagnosis and treatment. Operative Dentistry. 1979; 4:63–70. [PubMed: 296808]

150. Nakajima M, Sano H, Burrow MF, Tagami J, Yoshiyama M, Ebisu S, et al. Tensile bond strength and SEM evaluation of caries-affected dentin using dentin adhesives. Journal of Dental Research. 1995; 74:1679–1688. [PubMed: 7499591]

151. Yoshiyama M, Tay FR, Doi J, Nishitani Y, Yamada T, Itou K, et al. Bonding of self-etch and total-etch adhesives to carious dentin. Journal of Dental Research. 2002; 81:556–560. [PubMed: 12147747]

152. Scholtanus JD, Purwanta K, Dogan N, Kleverlaan CJ, Feilzer AJ. Microtensile bond strength of three simplified adhesive systems to caries-affected dentin. Journal of Adhesive Dentistry. 2010; 12:273–278. [PubMed: 20157668]

153. Neves, Ade A.; Coutinho, E.; Cardoso, MV.; de Munck, J.; Van Meerbeek, B. Micro-tensile bond strength and interfacial characterization of an adhesive bonded to dentin prepared by

contemporary caries-excavation techniques. Dental Materials. 2011; 27:552–562. [PubMed: 21489617]

154. Yoshiyama M, Tay FR, Torii Y, Nishitani Y, Doi J, Itou K, et al. Resin adhesion to carious dentin. American Journal of Dentistry. 2003; 16:47–52. [PubMed: 12744413]
155. Say EC, Nakajima M, Senawongse P, Soyman M, Ozer F, Tagami J. Bonding to sound vs caries-affected dentin using photo- and dual-cure adhesives. Operative Dentistry. 2005; 30:90–98. [PubMed: 15765963]
156. Ito S, Saito T, Tay FR, Carvalho RM, Yoshiyama M, Pashley DH. Water content and apparent stiffness of non-caries versus caries-affected human dentin. Journal of Biomedical Materials Research Part B, Applied Biomaterials. 2005; 72:109–116.
157. Zavgorodniy AV, Rohanizadeh R, Bulcock S, Swain MV. Ultrastructural observations and growth of occluding crystals in carious dentine. Acta Biomaterialia. 2008; 4:1427–1439. [PubMed: 18501691]
158. Perdigão J. Dentin bonding-variables related to the clinical situation and the substrate treatment. Dental Materials. 2010; 26:e24–e37. [PubMed: 20005565]
159. Kuboki Y, Ohgushi K, Fusayama T. Collagen biochemistry of the two layers of carious dentin. Journal of Dental Research. 1977; 56:1233–1237. [PubMed: 272387]
160. Deyhle H, Bunk O, Müller B. Nanostructure of healthy and caries-affected human teeth. Nanomedicine. 2011; 7:694–701. [PubMed: 21945898]
161. Ngo H. Glass-ionomer cements as restorative and preventive materials. Dental Clinics of North America. 2010; 54:551–563. [PubMed: 20630196]
162. Peters MC, Bresciani E, Barata TJ, Fagundes TC, Navarro RL, Navarro MF, et al. In vivo dentin remineralization by calcium-phosphate cement. Journal of Dental Research. 2010; 89:286–291. [PubMed: 20139340]
163. Sauro S, Thompson I, Watson TF. Effects of common dental materials used in preventive or operative dentistry on dentin permeability and remineralization. Operative Dentistry. 2011; 36:222–230. [PubMed: 21777102]
164. Poggio C, Lombardini M, Vigorelli P, Ceci M. Analysis of dentin/enamel remineralization by a CPP-ACP paste: AFM and SEM study. Scanning. 2013 [Epub ahead of print].
165. Koutsoukos PG, Nancollas GH. Crystal growth of calcium phosphates – epitaxial considerations. Journal of Crystal Growth. 1981; 53:10–19.
166. Jiang H, Liu XY. Principles of mimicking and engineering the self-organized structure of hard tissues. The Journal of Biological Chemistry. 2004; 297:41286–41293. [PubMed: 15192103]
167. Wong TS, Brough B, Ho CM. Creation of functional micro/nano systems through top- down and bottom-up approaches. Molecular & Cellular Biomechanics. 2009; 6:1–55. [PubMed: 19382535]
168. ten Cate JM, Damen JJ, Buijs MJ. Inhibition of dentin demineralization by fluoride in vitro. Caries Research. 1998; 32:141–147. [PubMed: 9544863]
169. ten Cate JM, van Duinen RN. Hypermineralization of dentinal lesions adjacent to glass-ionomer cement restorations. Journal of Dental Research. 1995; 74:1266–1271. [PubMed: 7629335]
170. Kawasaki K, Ruben J, Tsuda H, Huysmans MC, Takagi O. Relationship between mineral distributions in dentin lesions and subsequent remineralization in vitro. Caries Research. 2000; 34:395–403. [PubMed: 11014906]
171. Preston KP, Smith PW, Higham SM. The influence of varying fluoride concentrations on in vitro remineralisation of artificial dentinal lesions with differing lesion morphologies. Archives of Oral Biology. 2008; 53:20–26. [PubMed: 17920030]
172. Wang L, Nancollas GH. Pathways to biomineralization and biodemineralization of calcium phosphates: the thermodynamic and kinetic controls. Dalton Transactions. 2009; 15:2665–2672. [PubMed: 19333487]
173. Skrtic D, Antonucci JM, Eanes ED. Improved properties of amorphous calcium phosphate fillers in remineralizing resin composites. Dental Materials. 1996; 12:295–301. [PubMed: 9170997]
174. Skrtic D, Antonucci JM, Eanes ED, Eichmiller FC, Schumacher GE. Physiological evaluation of bioactive polymeric composites based on hybrid amorphous calcium phosphates. Journal of Biomedical Materials Research Part B, Applied Biomaterials. 2000; 53B:381–391.

175. Dickens SH, Flaim GM, Takagi S. Mechanical properties and biochemical activity of remineralizing resin-based Ca-PO_4 cements. Dental Materials. 2003; 19:558–566. [PubMed: 12837405]

176. Dickens SH, Flaim GM, Floyd CJE. Effect of resin composition on mechanical and physical properties of calcium phosphate filled bonding systems. Polymer Preprints. 2004; 45:329–330.

177. Xu HHK, Sun L, Weir MD, Antonucci JM, Takagi S, Chow LC. Nano dicalcium phosphate anhydrous-whisker composites with high strength and Ca and PO_4 release. Journal of Dental Research. 2006; 85:722–727. [PubMed: 16861289]

178. Xu HHK, Weir MD, Sun L, Takagi S, Chow LC. Effect of calcium phosphate nanoparticles on Ca-PO_4 composites. Journal of Dental Research. 2007; 86:378–383. [PubMed: 17384036]

179. Regnault WF, Icenogle TB, Antonucci JM, Skrtic D. Amorphous calcium phosphate/urethane methacrylate resin composites. I. Physicochemical characterization. Journal of Materials Science: Materials in Medicine. 2008; 19:507–515. [PubMed: 17619969]

180. Langhorst SE, O'Donnell JNR, Skrtic D. In vitro remineralization of enamel by polymeric amorphous calcium phosphate composite: Quantitative microradiographic study. Dental Materials. 2009; 25:884–891. [PubMed: 19215975]

181. Eanes ED. Amorphous calcium phosphate. Monographs in Oral Science. 2001; 18:130–147. [PubMed: 11758445]

182. Xu HHK, Moreau JL, Sun L, Chow LC. Nanocomposite containing amorphous calcium phosphate nanoparticles for caries inhibition. Dental Materials. 2011; 27:762–769. [PubMed: 21514655]

183. Moreau JL, Sun L, Chow LC, Xu HHK. Mechanical and acid neutralizing properties and inhibition of bacterial growth of amorphous calcium phosphate dental nanocomposite. Journal of Biomedical Materials Research Part B, Applied Biomaterials. 2011; 98B:80–88.

184. Melo MA, Cheng L, Weir MD, Hsia RC, Rodrigues LK, Xu HH. Novel dental adhesive containing antibacterial agents and calcium phosphate nanoparticles. Journal of Biomedical Materials Research Part B, Applied Biomaterials. 2013; 101:620–629.

185. Melo MA, Cheng L, Zhang K, Weir MD, Rodrigues LK, Xu HH. Novel dental adhesives containing nanoparticles of silver and amorphous calcium phosphate. Dental Materials. 2013; 29:199–210. [PubMed: 23138046]

186. Cochrane NJ, Reynolds EC. Calcium phosphopeptides -- mechanisms of action and evidence for clinical efficacy. Advances in Dental Research. 2012; 24:41–47. [PubMed: 22899678]

187. Cross KJ, Huq NL, Palamara JE, Perich JW, Reynolds EC. Physicochemical characterization of casein phosphopeptide-amorphous calcium phosphate nanocomplexes. The Journal of Biological Chemistry. 2005; 280:15362–15369. [PubMed: 15657053]

188. Bader JD. Casein phosphopeptide-amorphous calcium phosphate shows promise for preventing caries. Evidence Based Dentistry. 2010; 11:11–12. [PubMed: 20348890]

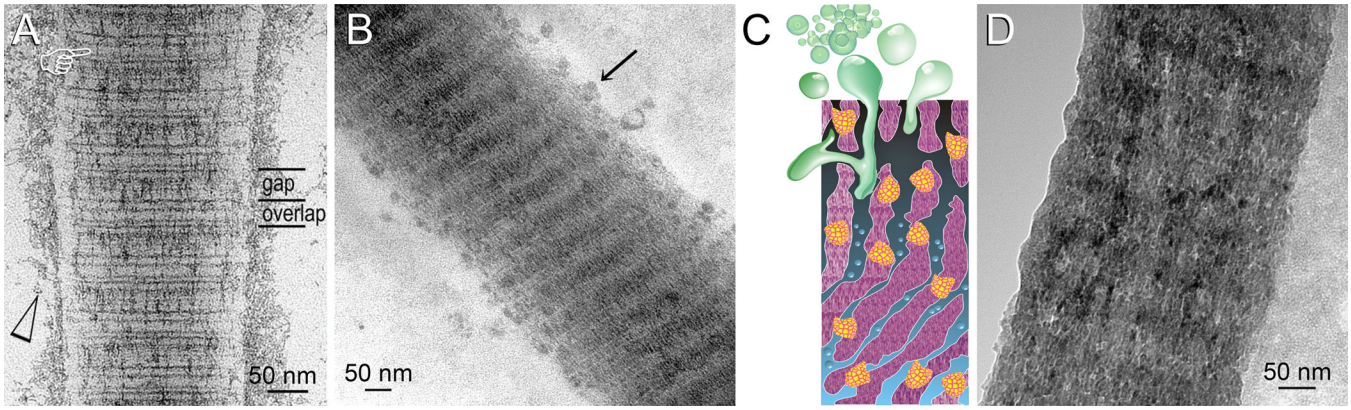

Figure 1.

A two-dimensional model for examining mineralization of reconstituted collagen fibrils, using a dual biomimetic analog mineralization protocol. Transmission electron microscopy (TEM) images of unsectioned reconstituted collagen fibrils. **A**. After 24 hours of mineralization. The fibril was briefly stained with uranyl acetate to highlight the gap and overlap zones. Amorphous calcium phosphate (ACP) prenucleation clusters (open arrowhead) could be seen along the periphery of the fibril. Pointer: initial needle-shaped intrafibrillar apatite. **B**. Unstained collagen fibril after 48 hours of mineralization. Prenucleation clusters have coalesced into ACP droplets (arrow) that continued to infiltrate the fibril. Denser intrafibrillar apatite deposition could be seen but the banding periodicity caused by hierarchical arrangement of the apatite crystallites was still present. **C**. Schematic depicting replacement of intrafibrillar water with fluidic polyacrylic acid-stabilized ACP nanoprecursors. **D**. Unstained fibril showing heavy intrafibrillar mineralization with apatite platelets after 72 hours. Banding characteristics was obscured by the heavy mineralization.

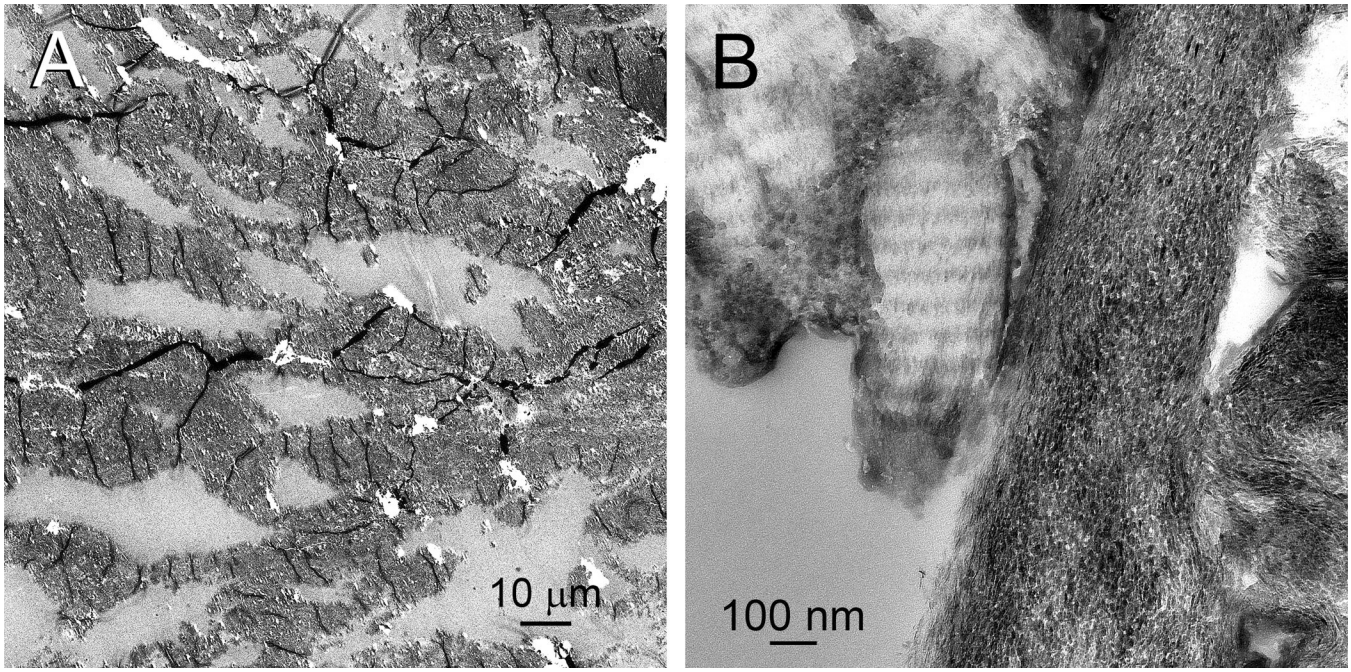

Figure 2.

A three-dimensional reconstituted collagen model of biomimetic mineralization. TEM images of an unstained section taken from a highly porous collagen scaffold that had been mineralized with a calcium and phosphate-containing medium containing dual biomimetic analogs for 14 days. **A**. Low magnification of the mineralized collagen scaffold, showing interconnecting mineralized collagen bundles. **B**. High magnification taken from a part of a mineralized collagen bundle. Collagen fibrils on the left are less heavily mineralized, with hierarchical deposition of apatite platelets in the gap zones, producing a periodic banding pattern. Collagen fibrils on the right are heavily mineralized with apatite platelets. Banding characteristic can no longer be identified.

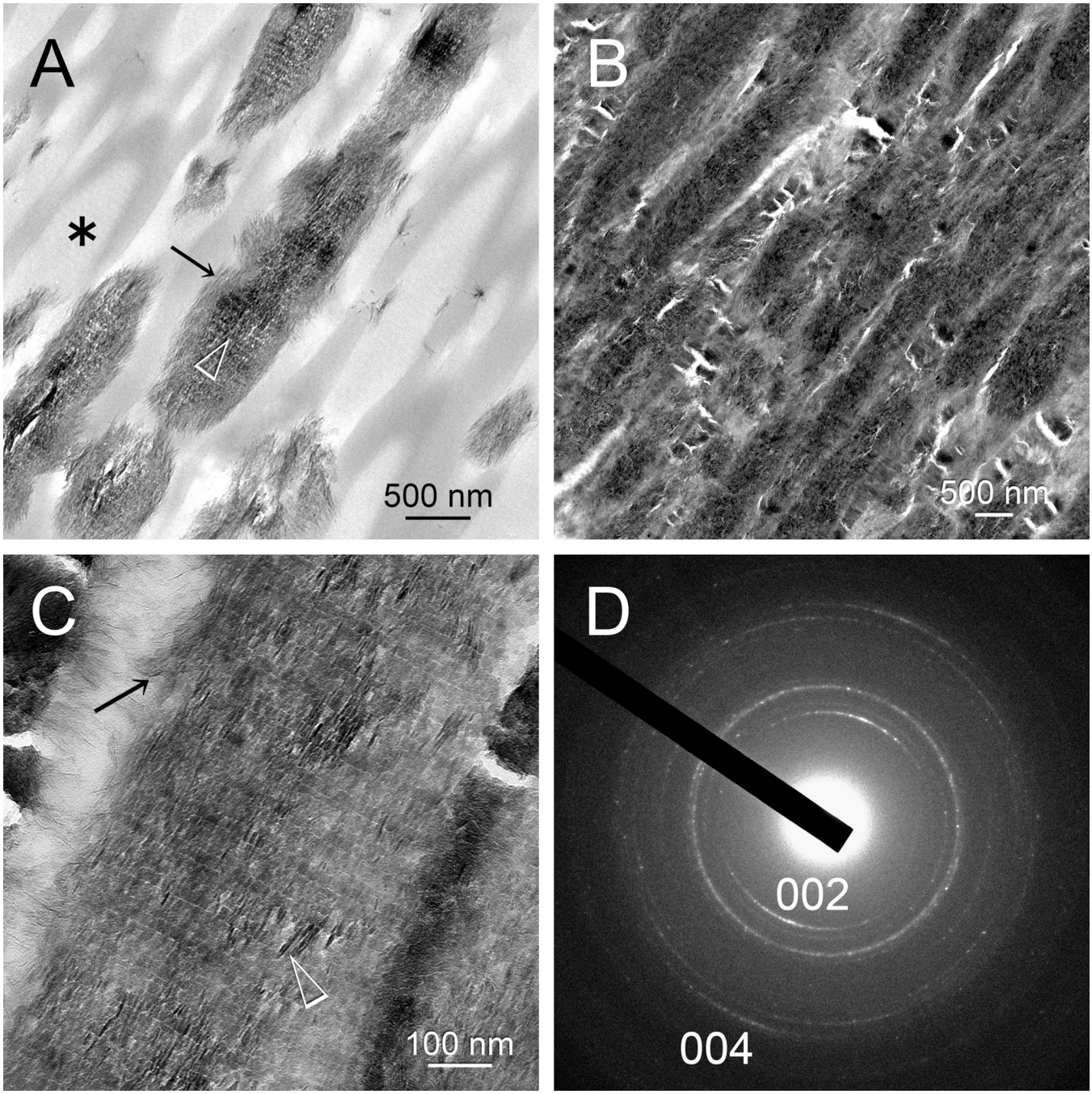

Figure 3.

A three-dimensional natural soft tissue collagen model of biomimetic mineralization. TEM images of unstained sections taken from mineralized rat tail tendon with parallel collagen fibrils at different time periods. **A**. Incomplete mineralization at 7 days. Asterisk: Unmineralized collagen fibrils; Arrow: extrafibrillar mineralization; Open arrowhead: Intrafibrillar mineralization recapitulating the **D**-spacings of fibrillar collagen. **B**. Heavy mineralization of the parallel collagen fibrils after 14 days. **C**. High magnification of B, showing a collagen fibril with extrafibrillar (arrow) and intrafibrillar mineralization by discrete apatite platelets (open arrowhead). **D**. Selected area electron diffraction of the

mineralized fibril in C produced arc-shaped diffraction patterns in the 002 and 004 plane of apatite. The C-axis of the apatite platelets are arranged almost parallel to the longitudinal axis of the collagen fibril.

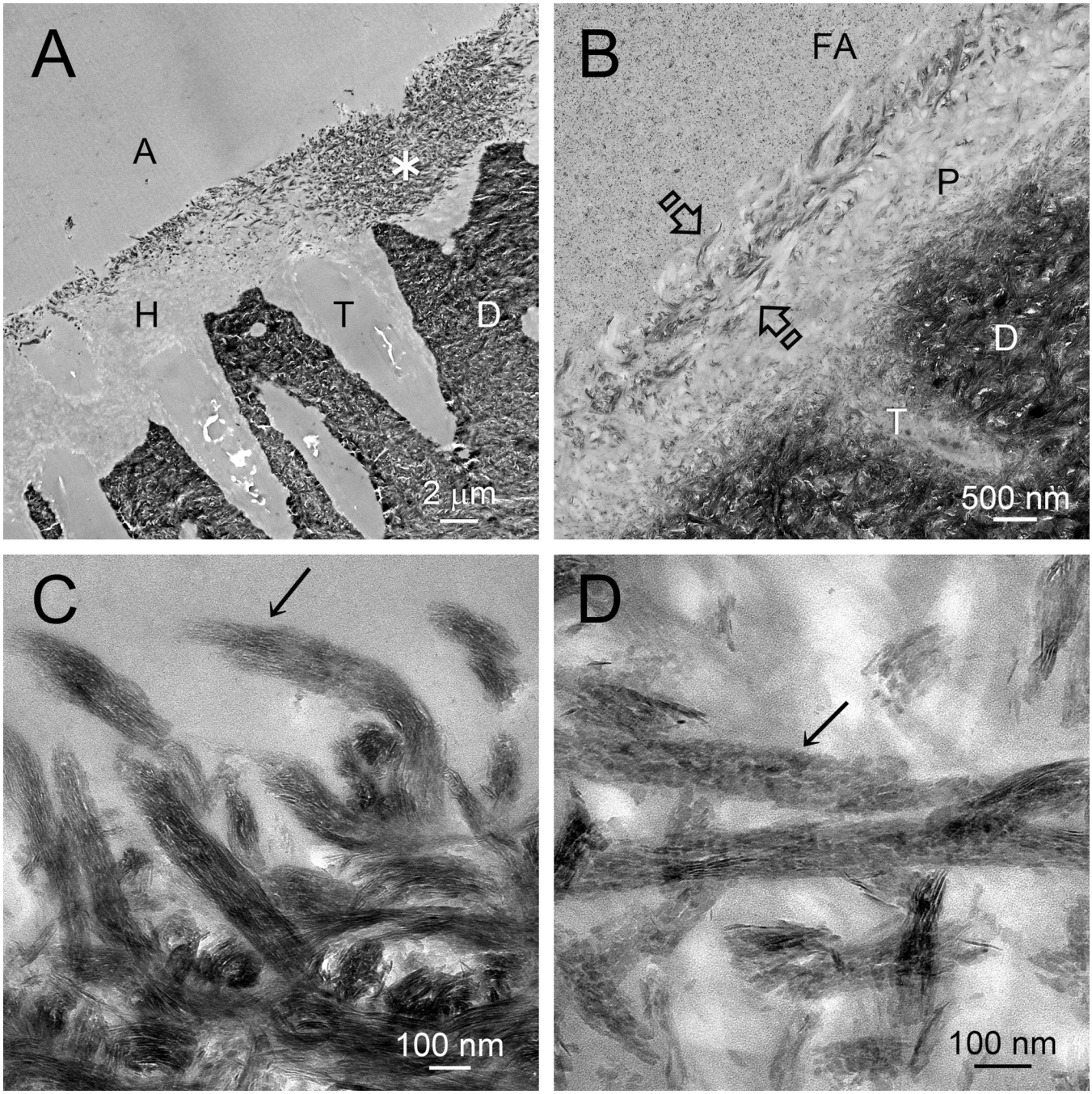

Figure 4.

Unstained TEM images illustrating biomimetic remineralization of hybrid layers created by **A**. An etch-and-rinse adhesive. A: adhesive; H: apatite-depleted hybrid layer created by phosphoric acid etching for 15 seconds; T: dentinal tubule; D: mineralized dentin; Asterisk: water-rich part of the hybrid layer remineralized by apatite crystallites. **B**. A moderately aggressive self-etch adhesive. FA: filled adhesive; P: partially-demineralized base of the hybrid layer; T: dentinal tubule; D: mineralized dentin; Between open arrows: water-rich surface of the hybrid layer remineralized by apatite crystallites. **C**. High magnification of the surface of a remineralized hybrid layer showing partially-unraveled surface collagen fibrils

in which their intrafibrillar compartments were filled with continuous strands of apatite mineral. **D**. High magnification image taken from the middle part of a remineralized hybrid layer showing collagen fibrils that were remineralized with discrete intrafibrillar apatite platelets.

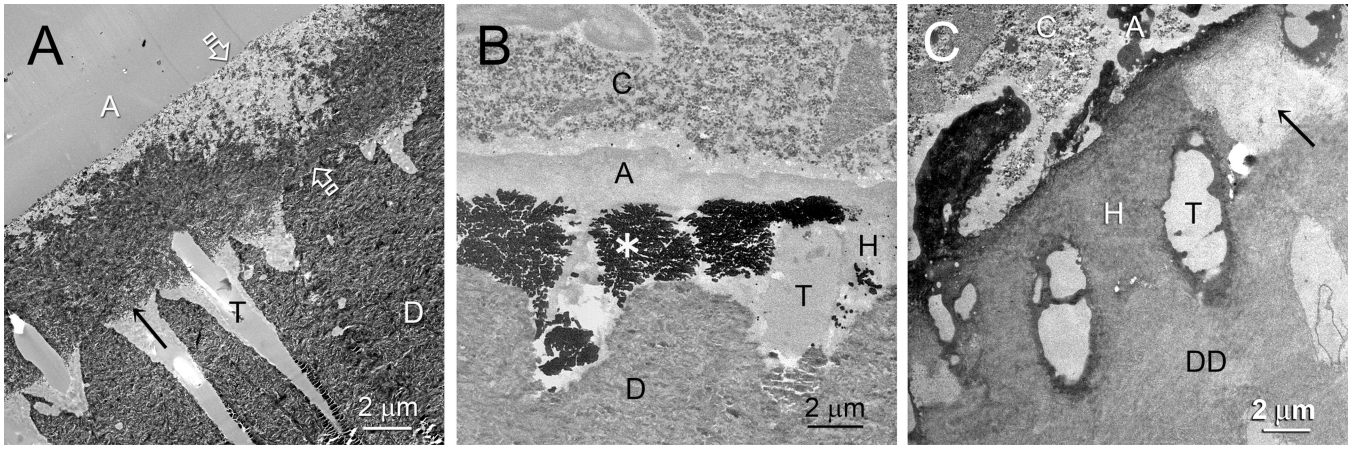

Figure 5.

Similarities in the ultrastructural manifestations of biomimetic remineralization; nanoleakage and degradation of aged hybrid layers created by etch-and-rinse adhesives. Abbreviations: C: resin composite; A: adhesive; H: hybrid layer; D: mineralized dentin base; DD: demineralized dentin base; T: dentinal tubule. **A**. Unstained mineralized section of a hybrid layer that had undergone biomimetic remineralization prior to aging for 12 months. Regions within the hybrid layer that were remineralized appear as electron-dense regions (arrow) within the unstained hybrid layer (between open arrowheads). **B**. Unstained mineralized section showing highly electron dense, extensive silver deposits (asterisk) within a hybrid layer that had been aged for 12 months prior to immersion in ammoniacal silver nitrate for nanoleakage evaluation. **C**. Stained demineralized section of the resin-dentin interface that had been aged for 12 months prior to laboratory processing. Part of the hybrid layer was degraded (arrow) and did not take up the staining observed in the non-degraded part of the hybrid layer.

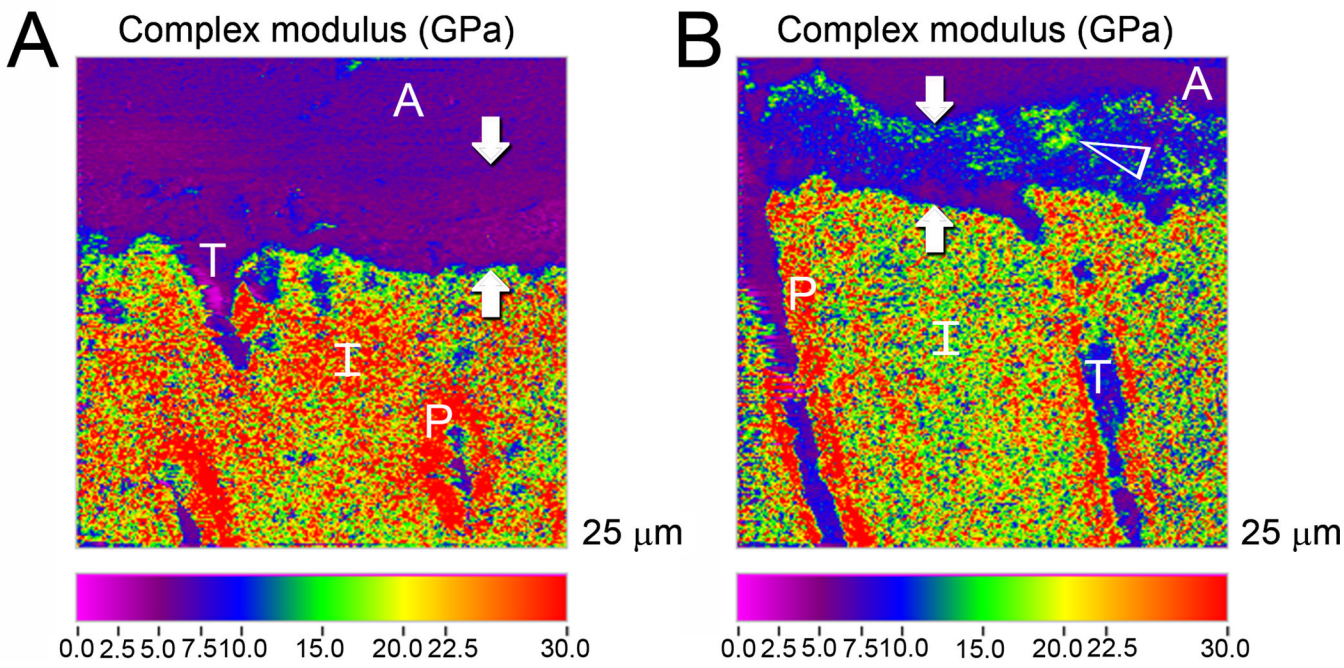

Figure 6.

Nanodynamic mechanical analysis and scanning probe microscopy of the resin dentin interface created by an etch–and-rinse adhesive **A**. before and **B**. after biomimetic remineralization. Only the complex modulus is shown. For Figure B, remineralized regions (open arrowhead) within the hybrid layer exhibit increases in the complex modulus. A: adhesive; Between solid arrows: hybrid layer; T: dentinal tubule; I: intertubular dentin: P: peritubular dentin.

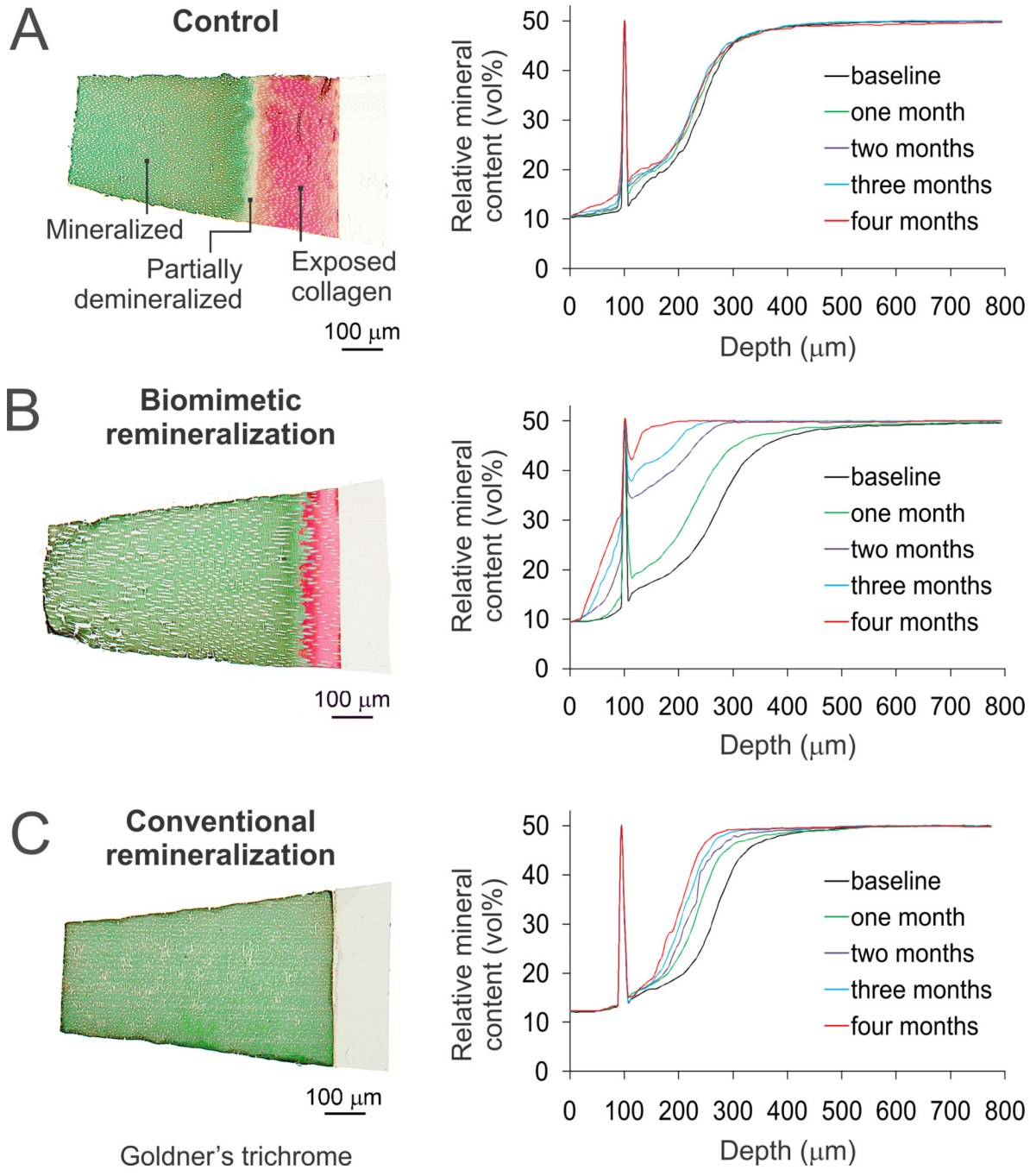

Figure 7.

Comparison of the status of remineralization of artificial caries-like lesions created in dentin over a 4 month period. For each figure, the light microscopy section on the left was stained with Goldner's trichrome; mineralized collagen was stained green while exposed collagen was stained red. The chart on the right represents the changes in overall mineral profile over time for the 250–300 μm thick artificial caries lesion, as determined by micro-computed tomography. **A**. Control (no remineralization after immersion in a non-mineralizing medium). **B**. Conventional remineralization (top-down approach) using a medium consisting of 1.5 mM $CaCl_2$, 0.9 mM KH_2PO_4, 130 mM KCl, 20 mM HEPES and 5 mM NaN_3**C**.

Biomimetic remineralization (bottom-up approach) using a medium consisting of 136.8 mM NaCl, 4.2 mM $NaHCO_3$, 3 mM KCl, 1 mM $K_2HPO_4 \cdot 3H_2O$, 1.5 mM $MgCl_2 \cdot 6H_2O$, 2.5 mM $CaCl_2$, 0.5 mM Na_2SO_4, 5 mM NaN_3, supplemented with 500 μg/mL polyacrylic acid and 200 μg/mL of polyvinylphosphonic acid. Set white Portland cement was used as the source of sustained calcium and hydroxyl ions release for initial formation of amorphous calcium phosphate nanoprecursors, in the presence of phosphate ions derived from the liquid medium.

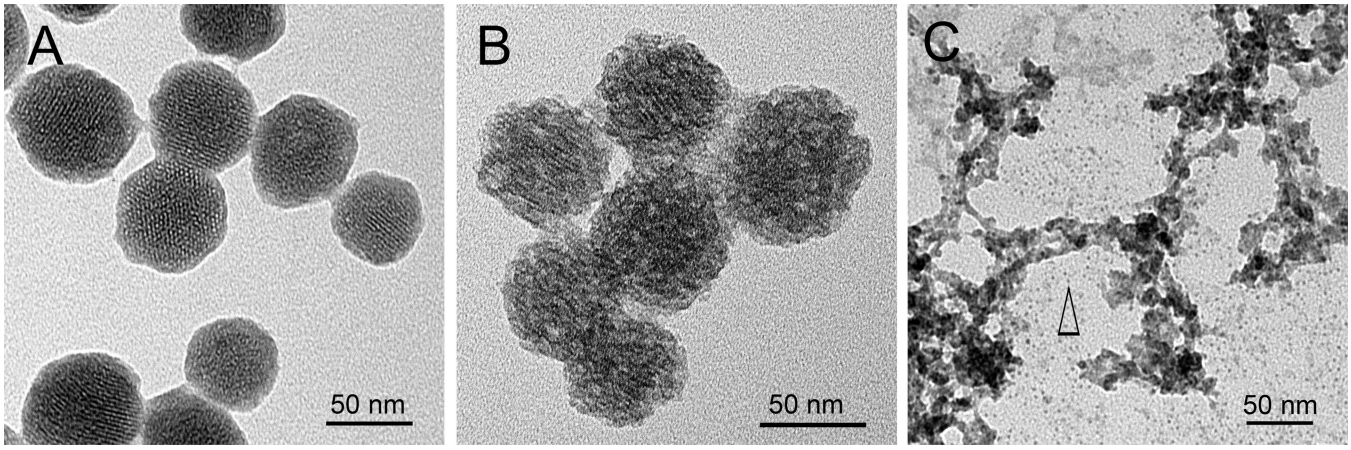

Figure 8.

Unstained TEM images of **A**. Mesoporous silica nanoparticles with a hexagonal array of mesopores. **B**. Loading of polyacrylic acid-stabilized amorphous calcium phosphate into the mesopores. **C**. Intentional dissolution of the silica framework of the loaded mesoporous silica nanoparticles in 0.05 N NaOH results in the release of amorphous calcium phosphate particles and prenucleation clusters (open arrowhead). Although the silica dissolution process is for removed from clinical application, the technique illustrates that the calcium phosphate phase within the mesoporous remains amorphous and has not been converted into apatite (selected area electron diffraction not shown).